2H, –CONH–CH_2–), 2.8–3.1 (m, 4H, por–CH_2–CH_2–), 3.2–3.3 (t, 2H, –CH_2–Im), 3.4 (s, 3H, –COO–CH_3), 3.5–3.8 (m, 12H, por–CH_3), 4.2–4.4 (t, 4H, por–CH_2–), 5.6–5.7 (d, 1H, Im), 5.8 (m, 1H, Im), 6.1–6.4 (q, 4H, =CH_2 (vinyl)), 8.1–8.2 (m, 2H, –CH= (vinyl)), 9.8–10.1 (m, 4H, *meso*); MS *m/z*: 709.72.

Fe(III) complex of 6a (6b). Iron insertion to **6a** was carried out by the same procedure as in the **1b** preparation. Yield 64%; R_f = 0.2 ($CHCl_3$/CH_3OH = 8/1); IR (NaCl) ν = 1732 (C=O, ester), 1652 (C=O, amide) cm^{-1}; UV-vis ($CHCl_3$) λ_{max} = 401, 580, 630 nm; HR-MS *m/z*: calcd. for $C_{43}H_{47}O_3N_7Fe$: 765.3090, found: 766.3184 [M + H^+].

3,18-Diethyl-8-(3-carboxy)ethyl-12-(3-(*N*-imidazolyl)propyl-amido)ethyl-2,7,13,17-tetramethylporphyrin (7a). Compound **7a** was synthesized by the same procedure as for **1a** except for using mesoporphyrin IX instead of protoporphyrin IX. Yield 10%; R_f: 0.4 ($CHCl_3$/CH_3OH = 20/1); IR (NaCl) ν = 1732 (C=O, ester), 1651 (C=O, amide) cm^{-1}; UV-vis ($CHCl_3$) λ_{max} = 408, 506, 542, 576, 630 nm; ^{1}H-NMR ($CDCl_3$) δ: 0.8 (m, 3H, CH_3–CH_2–O–), 1.6 (m, 2H,–CH_2–CH_2–Im), 1.8 (t, 6H, CH_3–CH_2–Por), 2.9 (m, 2H, CH_3–CH_2–O–), 3.1 (m, 4H, –CH_2–COO–), 3.2 (m, 2H, –NH–CH_2–), 3.6 (m, 12H, CH_3–Por), 3.8 (m, 2H,–CH_2–Im), 4.1 (m, 4H,CH_3–CH_2–Por), 4.4 (m, 4H, Por–CH_2–), 6.6 (s, 1H, –NHCO–), 6.0–6.8 (d, 3H, Im), 10.0 (m, 4H, *meso*); MS *m/z*: 699.32.

Fe(III) complex of 7a (7b). Iron insertion to **7a** was carried out by the same procedure as in the **1b** preparation. Yield 62%; R_f: 0.2 ($CHCl_3$/CH_3OH = 6/1); IR (NaCl) ν = 1732 (C=O, ester), 1668 (C=O, amide) cm^{-1}; UV-vis (DMF) λ_{max} = 394, 566, 591 nm; MS *m/z*: calcd for $C_{42}H_{49}O_3N_7Fe$: 755.3292, found 755.3246 [M^+].

3,18-Diacetyl-8-(3-carboxy)ethyl-12-(3-(*N*-imidazolyl)propyl-amido)ethyl-2,7,13,17-tetramethylporphyrin (8a). Compound **8a** was synthesized by the same procedure as for **1a** except for using diacetyldeuteroporphyrin IX instead of protoporphyrin IX. Yield 27%; R_f: 0.1 ($CHCl_3$/CH_3OH = 6/1); IR (NaCl) ν = 1735 (C=O, ester), 1651 (C=O, amide, ketone) cm^{-1}; UV-vis ($CHCl_3$) λ_{max} = 423, 516, 551, 586, 640 nm; ^{1}H-NMR ($CDCl_3$) δ: 1.5 (m, 2H, –CH_2–CH_2–Im), 2.9–3.1 (M, 4H, –CH_2–Im, –NH–CH_2–), 3.2–3.3 (m, 16H, –CH_2–COO, CH_3–Por), 3.4 (m, 6H, CH_3–CO–), 3.6 (m, 3H, CH_3–OCO–), 4.1 (m, 4H, Por–CH_2–), 6.0 (d, 1H, Im), 6.6 (m, 1H, Im), 6.9 (m, 1H, Im), 10 (m, 4H, *meso*); MS *m/z*: 712.

Fe(III) complex of 8a (8b). Iron insertion to **8a** was carried out by the same procedure as in the **1b** preparation. Yield 64%; R_f: 0.1 ($CHCl_3$/CH_3OH = 6/1); IR (NaCl) ν = 1735 (C=O, ester), 1651 (C=O, amide, ketone) cm^{-1}; UV-vis (DMF) λ_{max} = 418, 550, 578 nm; HR-MS *m/z*: calcd. for $C_{41}H_{43}O_5N_7Fe$: 769.2675, found 769.2697 [M^+].

Preparation of ferrous complex in DMF solution

The central Fe(III) ion of the porphyrin derivatives were reduced to the Fe(II) state using the complex of 18-crown-6 ether with $Na_2S_2O_4$ in DMF under aerobic conditions as previously reported.[8]

Preparation of rHSA–heme

Aqueous ascorbic acid (0.2 M, 10 μL) was added to an ethanol solution of the hemin derivative (2 mM, 1 mL) under a CO atmosphere. After complete reduction of the central Fe(III) ion, the ethanol solution (2 mM, 25 μL) was injected into the phosphate buffer solution (1 mM, pH 7.3, 2.5 mL) of rHSA (20 μM) under an Ar atmosphere. The formation of carbonyl rHSA–heme was confirmed by its UV-vis spectrum. The binding ratio of heme to rHSA was estimated by each concentration. The heme concentration was measured by the assay of iron ion using inductively coupled plasma spectrometry (Seiko, SPS7000A). The rHSA concentration was determined by bromocresol green along with the Albumin Test Wako kit (Wako Pure Chemical Industries).

Measurement of O_2 binding ability

The half-life of the O_2 adduct complex was determined by the time course of spectral changes, and the O_2 binding affinity ($P_{1/2}$) was determined by spectral changes at various partial pressures of O_2 according to previous reports.[2,15] rHSA–heme concentrations of 20 μM were normally used for UV-vis absorption spectroscopy. The spectra were recorded within the range of 350–700 nm.

Acknowledgements

This work was partially supported by a Grant-in-Aid for Scientific Research (No. 16350093) from JSPS, a Grant-in-Aid for Exploratory Research (No. 16655049) from MEXT Japan, and Health Science Research Grants from MHLW Japan.

References

1 (*a*) J. P. Collman, R. Boulatov, C. J. Sunderland and L. Fu, *Chem. Rev.*, 2004, **104**, 561; (*b*) M. Momenteau and C. A. Reed, *Chem. Rev.*, 1994, **94**, 659, and references therein.
2 T. Peters, Jr., *All about Albumin, Biochemistry, Genetics, and Medical Applications*, Academic Press, New York, 1996.
3 (*a*) T. Komatsu, K. Ando, N. Kawai, H. Nishide and E. Tsuchida, *Chem. Lett.*, 1995, 812; (*b*) T. Komatsu, K. Hamamatsu, J. Wu and E. Tsuchida, *Bioconjugate Chem.*, 1999, **10**, 82; (*c*) E. Tsuchida, T. Komatsu, Y. Mastukawa, K. Hamamatsu and J. Wu, *Bioconjugate Chem.*, 1999, **10**, 797; (*d*) T. Komatsu, T. Okada, M. Moritake and E. Tsuchida, *Bull. Chem. Soc. Jpn.*, 2001, **74**, 1695; (*e*) T. Komatsu, Y. Matsukawa and E. Tsuchida, *Bioconjugate Chem.*, 2002, **13**, 397; (*f*) A. Nakagawa, T. Komatsu, N. Ohmichi and E. Tsuchida, *Chem. Lett.*, 2003, **32**, 504.
4 A. Sumi, W. Ohtani, K. Kobayashi, T. Ohmura, K. Tokoyama, M. Nishida and T. Suyama, *Biotechnol. Blood Proteins*, 1993, **227**, 293.
5 (*a*) E. Tsuchida, T. Komatsu, Y. Matsukawa, A. Nakagawa, H. Sakai, K. Kobayashi and M. Suematsu, *J. Biomed. Mater. Res.*, 2003, **64A**, 257; (*b*) Y. Huang, T. Komatsu, A. Nakagawa, E. Tsuchida and S. Kobayashi, *J. Biomed. Mater. Res.*, 2003, **66A**, 292; (*c*) E. Tsuchida, T. Komatsu, K. Hamamatsu, Y. Matsukawa, A. Tajima, A. Yoshizu, Y. Izumi and K. Kobayashi, *Bioconjugate Chem.*, 2000, **11**, 46.
6 (*a*) P. R. Oritz de Montellano, *Curr. Opin. Chem. Biol.*, 2000, **4**, 221; (*b*) R. B. Frydman and B. Frydman, *Acc. Chem. Res.*, 1987, **20**, 250.
7 (*a*) C. K. Chang and T. G. Traylor, *J. Am. Chem. Soc.*, 1973, **95**, 8475; (*b*) C. K. Chang and T. G. Traylor, *J. Am. Chem. Soc.*, 1973, **95**, 8477; (*c*) C. K. Chang and T. G. Traylor, *Proc. Natl. Acad. Sci. USA*, 1975, **72**, 1975; (*d*) T. G. Traylor, C. K. Chang, J. Geibel, A. Berzinis, T. Mincey and J. Cannon, *J. Am. Chem. Soc.*, 1979, **101**, 6716; (*e*) J. Geibel, J. Cannon, D. Cambell and T. G. Traylor, *J. Am. Chem. Soc.*, 1978, **100**, 3575.
8 T. Mincey and T. G. Traylor, *Bioinorg. Chem.*, 1978, **9**, 409.
9 (*a*) *Porphyrins and Metalloporphyrins*, ed. K. M. Smith, Elsevier, Amsterdam, 1975; (*b*) M. Brunori, U. Saggese, G. C. Rotilio, E. Antonini and J. Wyman, *Biochemistry*, 1971, **10**, 1604.
10 G. H. Beaven, S.-H. Chen, A. D'albis and W. B. Gratzer, *Eur. J. Biochem.*, 1974, **41**, 539.
11 M. Rotenberg, S. Cohen and R. Margalit, *Photochem. Photobiol.*, 1987, **46**, 689.
12 T. G. Traylor, D. K. White, D. W. Cambell and A. P. Berzinis, *J. Am. Chem. Soc.*, 1982, **103**, 4932.
13 E. Monzani, L. Linati, L. Casella, L. D. Gioia, M. Favretto, M. Gullotti and F. Chillemi, *Inorg. Chim. Acta*, 1998, **273**, 339.
14 (*a*) E. Tsuchida, H. Nishide, Y. Sato and M. Kaneda, *Bull. Chem. Soc. Jpn.*, 1982, **55**, 1890; (*b*) K. Soai, A. Ookawa and K. Kato, *Bull. Chem. Soc. Jpn.*, 1982, **55**, 1671.
15 J. P. Collman, J. I. Brauman, B. L. Iverson, J. L. Sessler, R. M. Morris and Q. H. Gibson, *J. Am. Chem. Soc.*, 1983, **105**, 3052.

J|A|C|S
COMMUNICATIONS

Published on Web 10/19/2004

Dioxygenation of Human Serum Albumin Having a Prosthetic Heme Group in a Tailor-Made Heme Pocket

Teruyuki Komatsu,*,† Naomi Ohmichi,† Patricia A. Zunszain,‡ Stephen Curry,‡ and Eishun Tsuchida*,†

Advanced Research Institute for Science and Engineering, Waseda University, 3-4-1 Okubo, Shinjuku-ku, Tokyo 169-8555, Japan, and Department of Biological Sciences, Imperial College London, Huxley Building, South Kensington Campus, London SW7 2AZ, United Kingdom

Received July 4, 2004; E-mail: eishun@waseda.jp

Human serum albumin (HSA, MW = 66.5 kD) is the most abundant plasma protein in our bloodstream and serves as a transporter for small hydrophobic molecules such as fatty acids, bilirubin, and steroids.[1,2] Hemin dissociated from methemoglobin is also bound within a narrow D-shaped cavity in subdomain IB of HSA with an axial coordination of Tyr-161 and electrostatic interactions between the porphyrin propionates and a triad of basic amino acid residues (Figure 1).[3,4] In terms of the general hydrophobicity of the α-helical pocket, HSA potentially has features similar to the heme-binding site of myoglobin (Mb) or hemoglobin (Hb). However, even if one reduces the ferric HSA−hemin to obtain a ferrous complex, it is immediately oxidized by O_2. This is due to the fact that HSA lacks a proximal histidine, which enables the heme group to bind O_2.[3−5] We have shown that HSA incorporating tetraphenylporphinatoiron derivatives having a covalently linked axial-base can absorb O_2 under physiological conditions with a O_2 binding affinity similar to that of Hb.[6]

In this paper, we report for the first time the introduction of a proximal histidine into the subdomain IB of HSA by site-directed mutagenesis to construct a tailor-made heme pocket, which allows a reversible O_2 binding to the prosthetic heme group. Laser flash photolysis experiments revealed that this artificial hemoprotein appears to have two different geometries of the axial-imidazole coordination and shows rather low O_2 binding affinity.

We designed two recombinant HSA (rHSA) mutants, in which single or double mutations were introduced into subdomain IB: I142H [rHSA(A)] and I142H/Y161L [rHSA(B)] (Figure 1). Replacement of Y161 by histidine was not done because modeling experiments indicated that the distance from N_ϵ(H142) to Fe(heme) would be too great (>4 Å). In our mutants, the N_ϵ(H142)−Fe distance was estimated to be 2.31 Å (compared to 2.18 Å in Mb). The specific mutations were introduced into the HSA coding region in a plasmid vector (pHIL-D2 HSA) using the QuikChange (Stratagene) mutagenesis kit, and the mutants were expressed in the yeast species *Pichia pastoris*.[7] The rHSA(wild-type or mutants)−hemin complexes were prepared essentially according to our previously reported procedures, except that myristate was not added.[4] The resulting hemoproteins exhibited only a single band in SDS-PAGE.

In the absorption spectrum of the rHSA(wt)−hemin solution, the distinct charge-transfer (CT) band of Fe^{3+}−phenolate appeared at 625 nm.[8] A magnetic circular dichroism (MCD) spectrum showed a W-shaped feature in the Soret-band region.[9] These results imply the formation of a high-spin Fe^{3+} complex with the phenolate oxygen ligand of Y161, which is quite consistent with that found in the crystal structure.[3,4]

rHSA(B)−hemin did not exhibit the CT band because of the Y161L mutation and was easily reduced to the corresponding ferrous complex by adding a small molar excess amount of aqueous $Na_2S_2O_4$ under an Ar atmosphere. A single broad absorption band (λ_{max} = 559 nm) in the α,β region was very similar to that of deoxy Mb and indicated the formation of a five-N-coordinate Fe^{2+} complex (Figure 2).[10] The spectral pattern was unaltered in the temperature range of 0−25 °C. The shape of the asymmetric MCD spectrum also resembled that of deoxy Mb.[11] This suggests that the heme is accommodated into the tailor-made heme pocket with an axial coordination involving His-142.

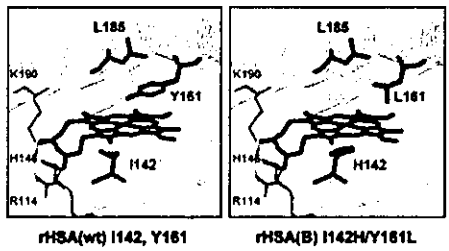

Figure 1. Prosthetic heme group complexed within the heme pocket in subdomain IB of rHSA(wt) and rHSA(B) mutant produced on the basis of the crystal structure coordinate of the rHSA−hemin complex (ref 4).

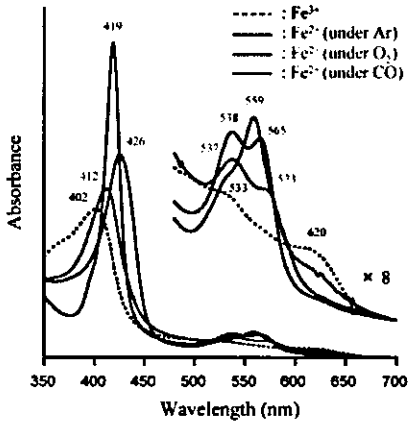

Figure 2. UV−vis absorption spectral changes of rHSA(B)−heme in phosphate buffered solution (pH 7.0, 50 mM) at 8 °C.

Upon exposure of the rHSA(B)−heme solution to O_2 gas, the UV−vis absorption changed to that of the dioxygenated complex (λ_{max} = 412, 537, 573 nm) at 0−25 °C[10] (lifetime of the O_2−adduct: ca. 10 min). After exposure to flowing CO, the heme produced a typical carbonyl complex (λ_{max} = 419, 538, 565 nm).

On the contrary, rHSA(A)−heme could not bind O_2 even at low temperature (~0 °C). It can be thought that the polar phenolate residue at the top of the porphyrin platform is likely to accelerate the proton-driven oxidation of the Fe^{2+} center. Replacing Y161 by

† Waseda University.
‡ Imperial College London.

10.1021/ja0460022t CCC: $27.50

Table 1. O_2 and CO binding Parameters of rHSA(B)−heme in Phosphate Buffered Solution (pH 7.0, 50 mM) at 22 °C

hemoprotein	k_{on}^{CO} (M^{-1} s^{-1})	$k_{on}^{O_2}$ (M^{-1} s^{-1})	$k_{off}^{O_2}$ (s^{-1})	$P_{1/2}^{O_2}$ (Torr)
rHSA(B)−heme[a]	2.0×10^6 (I), 2.7×10^5 (II)	7.5×10^6 (I and II)	221 (I), 1.7×10^3 (II)	18 (I), 134 (II)
Mb[b]	5.1×10^5	1.4×10^7	12	0.51
Hb (*R*-state)[c]	4.6×10^6	3.3×10^7	13	0.24

[a] Number in parentheses (I or II) indicates species I or II. [b] At 20 °C; ref 17. [c] At 20−21.5 °C; ref 18.

hydrophobic leucine greatly enhanced the stabilization of the O_2−adduct complex.

We then employed laser flash photolysis (Nd:YAG SHG; λ = 532 nm; 6 ns pulse width) to evaluate the kinetics of O_2 and CO bindings to rHSA(B)−heme.[12−14] Interestingly, the time dependence of the absorption change accompanying the CO recombination showed double-exponential profiles; the ratio of the amplitude of the fast and slow phases was always 3:2. On the other hand, the rebinding process of O_2 obeyed monophasic decay. On the basis of studies on synthetic model hemes, it has been shown that the proximal-side steric effect is the only primary factor that influences the association rate for CO but not for O_2.[12−14] One possible explanation is that there may be two different geometries of the axial His-142 coordination and that each one shows the individual kinetics of the CO rebinding. Marden and co-workers also found a similar behavior in CO association with HSA−heme and interpreted it as indicating that there are two orientations of the heme plane in the albumin scaffold.[5] In our case, the alternative geometries may arise because the heme molecule binds into the pocket of subdomain IB in two orientations related by a 2-fold rotation about its center (180° rotational isomers). Asymmetric 3,8-divinyl groups at the porphyrin periphery, in particular, would occupy different positions that result in a small divergence of the porphyrin ring and its iron center. The crystal structure analyses could not resolve this ambiguity, because the two configurations exist as a mixture.[3,4]

Our hypothesis is consistent with infrared spectroscopy data. The CO coordinated with rHSA(B)−heme showed a broad ν_{CO} at 1962 cm^{-1} with a shoulder at 1942 cm^{-1}. We therefore suggest that there are two different modes of π-back-donation from the central Fe^{2+} to the bound CO. It is remarkable that the lower stretching frequency is very close to that of Mb (ν_{CO} = 1943 cm^{-1}).[15] Attempts to determine the ratio of the two hemin orientations by ^1H NMR spectroscopy unfortunately failed.[16] The downfield spectra of rHSA(B)−hemin in met and met-azido forms did not show sharp resonances of the four porphyrin CH_3 groups.

The two geometries of the His-142 ligation in rHSA(B)−heme should yield two different O_2 binding affinities. By analyzing CO/O_2 competitive binding following laser flash photolysis, we obtained the association and dissociation rate constants for O_2 ($k_{on}^{O_2}$, $k_{off}^{O_2}$), and the O_2 binding affinities ($P_{1/2}^{O_2}$) for these two species (I and II) (Table 1).[12−14] The $P_{1/2}^{O_2}$ values were determined to be 18 and 134 Torr, respectively; this means that the O_2 binding affinities were 2.8 and 0.4%, respectively, of that observed for Mb.[17,18] Kinetically, for species I with $P_{1/2}^{O_2}$ of 18 Torr, an 18-fold increase in the $k_{off}^{O_2}$ value leads to the low affinity for O_2. Repeated studies with synthetic model hemes and engineered mutants of Mb or Hb have shown that low polarity of the microenvironment around the heme site decreases the O_2-binding affinity by increasing the dissociation rate constant.[12−14,17] In this albumin-based hemoprotein, the porphyrin ring is buried in the core of the pocket entirely made of hydrophobic residues. Therefore, the O_2 binding affinity becomes significantly lower than those of Mb and Hb. In species II with $P_{1/2}^{O_2}$ of 134 Torr, the proximal pull effect could further increase the $k_{off}^{O_2}$ value and may cause a large decline in the O_2 binding affinity.

We have recently found that heme is accommodated into the different architecture of a tailor-made heme pocket in rHSA (Y161L/L185H) [rHSA(C)] and that the rHSA(C)−heme complex also binds O_2 as well. In this case, the proximal histidine coordinates with the heme plane from the roof side, and the O_2 molecule binds from the floor side (Figure 1). Our combined structural and mutagenic approach allows us to significantly enhance the O_2 binding properties of rHSA−heme complexes and thereby mimic the diverse biological reactivities of natural hemoproteins. From the viewpoint of clinical applications, "O_2-carrying plasma albumin" could be of extreme medical importance not only for red blood cell substitutes but also for O_2-therapeutic reagents. The crystal structure analysis of this new class of artificial hemoproteins is now underway.

Acknowledgment. This work was partially supported by a Grant-in-Aid for Scientific Research (No. 16350093) from JSPS, a Grant-in-Aid for Exploratory Research (No. 16655049) from MEXT Japan, Health Science Research Grants (Regulatory Science) from MHLW Japan, and the Wellcome Trust (UK).

Supporting Information Available: Time dependence of the absorption change accompanying the CO or O_2 rebinding to rHSA(B)−heme after the laser flash photolysis (PDF). This material is available free of charge via the Internet at http://pubs.acs.org.

References

(1) Peters, T. *All about Albumin: Biochemistry, Genetics and Medical Applications*; Academic Press: San Diego, 1996.
(2) Curry, S.; Madelkow, H.; Brick, P.; Franks, N. *Nat. Struct. Biol.* **1998**, *5*, 827.
(3) Wardell, M.; Wang, Z.; Ho, J. X.; Robert, J.; Ruker, F.; Rubel, J.; Carter, D. C. *Biochem. Biophys. Res. Commun.* **2002**, *291*, 813.
(4) Zunszain, P. A.; Ghuman, J.; Komatsu, T.; Tsuchida, E.; Curry, S. *BMC Struct. Biol.* **2003**, *3*, 6.
(5) Marden, M. C.; Hazard, E. S.; Leclerc, L.; Gibson, Q. H. *Biochemistry* **1989**, *28*, 4422.
(6) Komatsu, T.; Matsukawa, Y.; Tsuchida, E. *Bioconjugate Chem.* **2002**, *13*, 397.
(7) Peterson, C. E.; Ha, C. E.; Harohalli, K.; Park, D.; Bhagavan, N. V. *Biochemistry* **1997**, *36*, 7012.
(8) Adachi, S.; Nagano, S.; Watanabe, Y.; Ishimori, K.; Morishima, I. *Biochem. Biophys. Res. Commun.* **1991**, *180*, 138.
(9) Pond, A. E.; Roach, M. P.; Sono, M.; Rux, A. H.; Franzen, S.; Hu, R.; Thomas, M. T.; Eilks, A.; Dou, Y.; Ikeda-Saito, M.; Oritz de Montellano, P. R.; Woodruff, W. H.; Boxer, S. G.; Dawson, J. H. *Biochemistry* **1999**, *38*, 7601.
(10) Antonini, E.; Brunori, M. In *Hemoglobin and Myoglobin in Their Reactions with Ligands*; North-Holland Publishing: Amsterdam, 1971; p 18.
(11) Vickrey, L.; Nozawa, T.; Sauer, K. *J. Am. Chem. Soc.* **1976**, *98*, 343.
(12) Collman, J. P.; Brauman, J. I.; Iverson, B. L.; Sessler, J. L.; Moris, R. M.; Gibson, Q. H. *J. Am. Chem. Soc.* **1983**, *105*, 3052.
(13) Traylor, T. G.; Tsuchiya, S.; Campbell, D.; Mitchel, M.; Stynes, D.; Koga, N. *J. Am. Chem. Soc.* **1985**, *107*, 604.
(14) Komatsu, T.; Arai, K.; Nishide, H.; Tsuchida, E. *J. Chem. Soc., Dalton Trans.* **1993**, 1734.
(15) Maxwell, J. C.; Volpe, J. A.; Barlow, C. H.; Caughey, W. S. *Biochem. Biophys. Res. Commun.* **1974**, *58*, 166.
(16) (a) Jue, T.; Krishnamoorthi, R.; La Mar, G. N. *J. Am. Chem. Soc.* **1983**, *105*, 5701. (b) Yamamoto, Y.; La Mar, G. N. *Biochemistry* **1986**, *25*, 5288.
(17) Olson, J. S.; Mathews, A. J.; Rohlfs, R. J.; Springer, B. A.; Egeberg, K. D.; Sliger, S. G.; Tame, J.; Renaud, J.-P.; Nagai, K. *Nature* **1988**, *336*, 265.
(18) (a) Gibson, Q. H. *J. Biol. Chem.* **1970**, *245*, 1564. (b) Olson, J. S.; Melvin, E.; Andersen, E.; Gibson, Q. H. *J. Biol. Chem.* **1971**, *246*, 5919. (c) Steinmeier, R. C.; Parkhurst, L. J. *Biochemistry* **1975**, *14*, 1564.

JA046022T

Exchange transfusion with synthetic oxygen-carrying plasma protein "albumin-heme" into an acute anemia rat model after seventy-percent hemodilution

Teruyuki Komatsu,[1] Hisashi Yamamoto,[2] Yubin Huang,[1] Hirohisa Horinouchi,[3] Koichi Kobayashi,[3] Eishun Tsuchida[1]

[1]*Advanced Research Institute for Science and Engineering, Waseda University, 3-4-1 Okubo, Shinjuku-ku, Tokyo 169-8555, Japan*

[2]*Pharmaceutical Research Center, NIPRO Corporation, 3023 Nojimachi, Kusatsu-shi, Shiga 525-0055, Japan*

[3]*Department of General Thoracic Surgery, School of Medicine, Keio University, 35 Shinanomachi, Shinjuku-ku, Tokyo 160-8582, Japan*

Received 22 July 2004; Accepted 5 August 2004
Published online 27 October 2004 in Wiley InterScience (www.interscience.wiley.com). DOI: 10.1002/jbm.a.30200

Abstract: Recombinant human serum albumin (rHSA) incorporating the synthetic heme "albumin-heme" is an oxygen-carrying plasma protein that has the potential to be a red blood cell substitute. The physiological responses to a 30% exchange transfusion with two types of albumin-heme (rHSA-FecycP, rHSA-FepivP) solutions after 70% isovolemic hemodilution with 5 g/dL rHSA were investigated using anesthetized rats. The circulation parameters, blood parameters, renal cortical oxygen pressure (pO_2), and muscle tissue pO_2 were carefully monitored for 60 min after the injection. The declined mean arterial pressure and the mixed venous partial pO_2 significantly recovered to 70.8 and 91.9% of the basal values by intravenous infusion of albumin-hemes, respectively. The lowered renal cortical pO_2 also increased, indicating oxygen transport by this synthetic hemoprotein. The administration of albumin-heme into the acute anemia rat model after hemorrhage improved the circulatory volume and resuscitated the shock state. Both rHSA-FecycP and rHSA-FepivP transported oxygen through the body. © 2004 Wiley Periodicals, Inc. J Biomed Mater Res 71A: 644–651, 2004

Key words: exchange transfusion; entirely synthetic oxygen-carrier; hemoprotein; albumin-heme; red blood cell substitute

INTRODUCTION

Because the risk of transmission of viral illness by transfused blood has become extremely low, transfusion of donor blood has nowadays become a routine procedure. However, this level of safety has been achieved at great cost, and the hepatitis virus or unknown infectious pathogens cannot be completely excluded by the nucleic acid test system. Furthermore, (i) the transfusion of donor blood requires cross-matching and compatibility tests to avoid the consequences of a hemolytic reaction in the recipient, and (ii) the purified red blood cells (RBCs) should be stored at 4°C. These requirements substantially limit the availability of blood in a disaster or emergency. Under this background, several types of hemoglobin (Hb)-based oxygen carriers have been studied as an RBC substitute or oxygen therapeutic agent.[1–4] Nevertheless, these materials do not fulfill all the requirements of blood replacement compositions. The first concern is the source of human Hb, which is limited by the availability of outdated human blood. Animal blood will raise anxiety of transmission of animal pathogens; for instance, bovine Hb may harbor prions. The Hb products potentially carry risks because of the biological origin of the raw materials. Additional problems of Hb-based oxygen carriers (i.e., modified Hb) are the high colloid osmotic pressure[5] and its vasopressor effect, which increase blood pressure and decrease cardiac output.[6–8] Although diaspirin intramolecularly crosslinked Hb is no longer developed, half of the products in advanced clinical trials still showed vasoconstriction.[4] The precise mechanism of

Correspondence to: E. Tsuchida; e-mail: eishun@waseda.jp
Contract grant sponsor: Health Science Research Grants (Regulatory Science) of the MHLW
Contract grant sponsor: JSPS Grant-in-Aid for Scientific Research; contract grant number: 16350093
Contract grant sponsor: MEXT Grant-in-Aid for Exploratory Research; contract grant number: 16655049

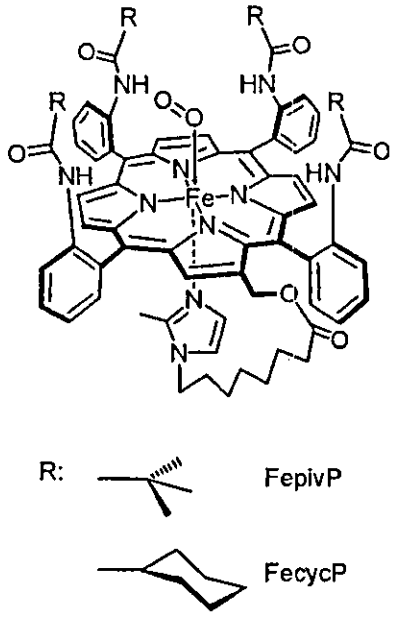

Chart 1

this hypertension is controversial, but many investigators suspect that the small Hb molecules penetrate the vascular endothelium and capture the endothelial-derived relaxing factor, namely, nitric oxide. In fact, glutaraldehyde crosslinked human polyHb does not show vasoactivity.[9] Others believe that the excessive delivery of oxygen to arteriolar vascular walls induces autoregulatory vasoconstriction.[10-13]

We have prepared entirely synthetic oxygen carriers without Hb. The incorporation of synthetic heme, 2-[8-{*N*-(2-methylimidazolyl)}octanoyloxymethyl]-5,10,15,20-tetrakis(α,α,α,α-*o*-pivalamidophenyl)porphinatoiron(II) (FepivP, Chart 1), into recombinant human serum albumin (rHSA) provides an artificial hemoprotein (rHSA-heme; rHSA-FepivP) that can reversibly bind and release oxygen under physiological conditions (pH 7.3, 37°C) like Hb.[14-19] An FepivP analog, 2-[8-{*N*-(2-methylimidazolyl)}-octanoyloxymethyl]-5,10,15,20-tetrakis{α,α,α,α-*o*-(1-methylcyclohexanamido)phenyl}porphinatoiron(II) (FecycP, Chart 1), which contains more hydrophobic 1-methylcyclohexanoyl fences, is also included into rHSA as well and the obtained rHSA-FecycP hybrid showed the same oxygen-binding equilibrium and a longer lifetime ($\tau_{1/2}$) of the oxy species compared with that of rHSA-FepivP.[20] The physicochemical properties and oxygen-transporting ability of these rHSA-based oxygen carriers, which are free of infectious pathogens, satisfy the initial clinical requirements as an RBC substitute. It is remarkable that the colloid osmotic pressure of 5 g/dL rHSA, rHSA-FecycP, and rHSA-FepivP are all the same.[15] We herein report the systematic evaluations of the physiological responses to exchange transfusions with two types of albumin-heme solutions, rHSA-FecycP and rHSA-FepivP, in anesthetized rats. The animals were first placed into an acute anemia induced by 70% hemodilution and then underwent a 30% exchange transfusion with albumin-hemes. Circulation parameters and blood parameters were monitored for 60 min after the injection. The *in vivo* oxygen deliveries to the renal cortex and the muscle tissue were also measured.

MATERIALS AND METHODS

Preparation of rHSA-heme solutions

The rHSA (Albrec®, 25 wt %) was obtained from NIPRO Corp. (Osaka, Japan). The 5 g/dL rHSA was made by diluting Albrec® with saline solution (Otsuka Pharmaceutical Co., Ltd.). Two types of albumin-hemes (rHSA-FecycP and rHSA-FepivP [rHSA]: approximately 5 g/dL) used for the exchange transfusions were prepared according to our previously reported procedure with some modifications.[19] The characteristics of these oxygen-carrying fluids are almost identical (Table I) except for the stability of the oxygenated species; oxy rHSA-FecycP showed a 4.5-fold longer lifetime against autooxidation than that of oxy rHSA-FepivP at 37°C *in vitro*. These red-colored albumin-heme solutions were filtered using a DISMIC 25CS045AS just before use.

Hemodilution and exchange transfusion

The investigations were performed according to our previously reported experimental protocols with 24 male Wistar rats (312 ± 2.9 g) (Scheme 1).[21] All animal handling and care were in accordance with the National Institutes of Health guidelines. The protocol details were approved by the Animal Care and Use Committee of Keio University.

The animals were placed on a heating pad under an inhalation anesthesia with sevoflurane; its concentration was kept at 2.0% for the operations and 1.5% for the experiments. After an incision was made in the neck, the heparinized catheter (Natume Seisakusho SP-55) was introduced into the right common carotid artery for blood withdrawal. Other catheters (SP-31) were also inserted into the left femoral artery for continuous mean arterial pressure (MAP) monitoring, and the right femoral vein for sample injection.

TABLE I
Characteristics of the Albumin-Heme Solutions

	rHSA-FecycP	rHSA-FepivP
pH	7.45	7.46
Viscosity (cP)	1.1	1.1
Heme (m*M*)	2.8	2.7
Met-heme content (%)	0	0
rHSA (%)	4.9	4.9
*p*50 (mmHg) at 37°C	37	32

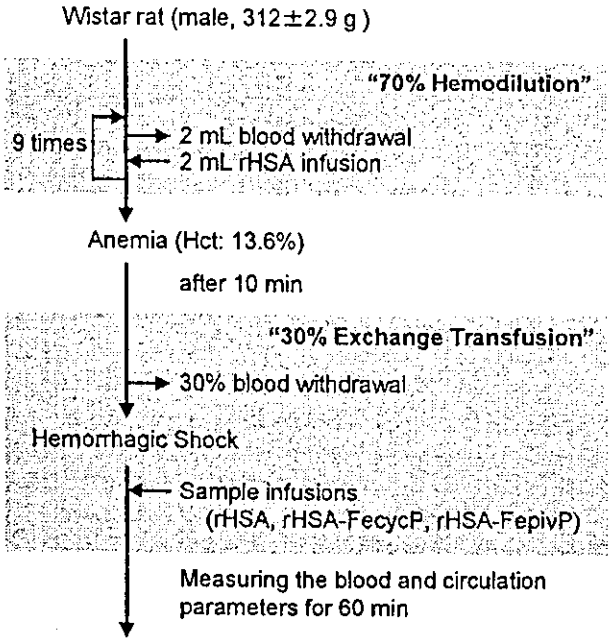

Scheme 1. Diagram illustrating the exchange, bleeding procedures, and materials.

Polarographic oxygen-electrodes (Intermedical POE-10N and POE-40PS) were inserted into the left renal cortex and muscle in the abdomen. Core temperature was measured with a rectal thermometer (Technol Seven D617-1).

After stabilization of the animal's condition, isovolemic 70% hemodilution was performed using 5 g/dL rHSA solution. Blood withdrawal via the common carotid artery (2 mL) and rHSA infusion from the femoral vein (2 mL) (each 1 mL/min) were repeated for nine cycles until the hematocrit (Hct) was reduced to 13.6% (32% of the initial Hct value: 42.6%). After 10 min, a 30% volume of the circulatory blood was withdrawn, producing a severe hemorrhagic shock state. The same volume of the samples (rHSA-FecycP and rHSA-FepivP) was then intravenously (iv) injected (n = 6 each). As negative- or positive-control groups, rats were infused with the 5 g/dL rHSA solution or the shed rat blood ([heme] = 5.3 m*M*) (rHSA group and whole blood group, n = 6 each). A blood-taking from the artery (0.3 mL) and vein (0.2 mL) was performed at the following six points: (i) before the 70% hemodilution, (ii) immediately after the hemodilution, and (iii) 10 min after the hemodilution, (iv) immediately after the 30% bleeding, (v) immediately after the sample infusion, and (vi) 60 min after the sample infusion. The animals were sacrificed after the experiments by sodium pentobarbital overdose. MAP was monitored through the femoral artery catheter connected to a transducer (NIHON KODEN TP-400 T or Becton Dickinson P23XL) with a pressure coupler and an amplifier (NIHON KODEN PP-101H and AP-100H). An electrocardiogram was measured using a bioelectric coupler and an amplifier (NIHON KODEN PC-101H and AC-100H), and heart rate (HR) was obtained from its R wave. MAP and HR were recorded by a Polygraph System (NIHON KODEN LEG-1000 version 01-02 or PEG-1000 version 01-01) at the following eight points: (i) before the 70% hemodilution, (ii) immediately after the hemodilution, (iii) 10 min after the hemodilution, (iv) immediately after the 30% bleeding, (v) immediately after the sample infusion, (vi) 5 min, (vii) 30 min, and (viii) 60 min after the sample infusion. The renal cortical oxygen-tension [ptO_2(R)] and muscle tissue oxygen-tension [ptO_2(M)] were simultaneously measured with a tissue oxygen-pressure monitor (Inter Medical PO_2-100DW) using an oxygen electrode (described above). Withdrawn blood was rapidly applied to a blood gas system (Radio Meter Trading ABL555) to measure the oxygen pressure (paO_2), pH and carbon dioxide pressure ($paCO_2$) of the arterial blood, and the oxygen pressure (pvO_2) of the venous blood. The RBC numbers were counted for the mixture of arterial blood (30 μL) and ACD-A solution using a multisystem automatic blood cell counter (Sysmex KX-21).

Data analysis

MAP, HR, respiration rate, paO_2, pvO_2, ptO_2(R), ptO_2(M), and $paCO_2$ are represented by percent ratios of the basal values as mean ± standard error of mean (SEM). Body temperature, pH, RBC numbers, and body weight are denoted by mean ± SEM.

Statistical analyses were performed using the Tukey-Kramer multiple comparison test for more than three groups [pH, RBC numbers, body weight, MAP, HR, respiration rate, paO_2, pvO_2, ptO_2(R), ptO_2(M), and $paCO_2$], and by repeated-measures analysis of variance followed by paired t test for comparison with a basal value (body temperature). Values of $p < 0.05$ were considered significant. The statistical analytic software used was StatView (SAS Institute Inc.).

RESULTS

Blood parameters

The basal values of several measurements, for which data are shown in percent ratios, are summarized in Table II. There are no significant differences in the four groups.

The 70% hemodilution decreased the Hct to 12.8–14.3% and RBC numbers to 202.2–223.2 × 10^4/μL, leading to acute anemia [Fig. 1(a,b)]. By a further 30% exchange transfusion with the whole blood of rat, both parameters slightly increased to 14.3% and 229.7 × 10^4/μL, respectively. They remained constant during the experimental period. In the rHSA-FecycP and rHSA-FepivP groups, both parameters decreased to 7.8–9.6% and 129.2–149.2 × 10^4/μL by the sample replacement. They corresponded well to the calculated values.

Survival time

After the exchange transfusion with the 5 g/dL rHSA solution (rHSA group), all animals died within 32 min;

TABLE II
Basal Values of Each Group

	rHSA	Whole blood	rHSA-FecycP	rHSA-FepivP
MAP (mmHg)	110 ± 2.9	115 ± 3.4	101 ± 7.3	107 ± 4.8
HR (beats/min)	371 ± 14	379 ± 17	380 ± 22	349 ± 10
Respiration rate (breaths/min)	66 ± 3.2	67 ± 4.4	60 ± 2.3	64 ± 1.7
ptO_2(R) (mmHg)	29.2 ± 2.8	38.5 ± 2.6	31.7 ± 3.6	30.2 ± 4.3
ptO_2(M) (mmHg)	39.8 ± 3.6	38.5 ± 3.7	44.2 ± 4.6	42.7 ± 3.9
paO_2 (mmHg)	83.8 ± 2.3	84.2 ± 2.3	87.8 ± 2.6	81.7 ± 2.2
pvO_2 (mmHg)	47.9 ± 1.6	46.8 ± 1.9	48.2 ± 3.1	47.4 ± 1.1
$paCO_2$ (mmHg)	42.0 ± 0.9	40.2 ± 0.8	39.6 ± 1.2	41.7 ± 1.0
Body weight (g)	312 ± 3.5	312 ± 3.9	311 ± 3.4	314 ± 0.8

the average survival time was 14.9 ± 4.3 min. However, all animals survived >60 min in the rHSA-FecycP, rHSA-FepivP, and whole blood groups. The body temperatures remained constant throughout the measurements (rHSA-FecycP group: 36.1°–36.6°C; rHSA-FepivP group: 36.3°–36.7°C; whole blood groups: 36.2°–36.8°C).

MAP, HR, and respiration rate

The 70% hemodilution decreased MAP to 77.4–81.9% of the basal value, and the further 30% bleeding decreased it to 24.9–37.7% of the baseline [Fig. 2(a)]. In contrast to the fact that no recovery was observed by the iv administration of 5 g/dL rHSA, the lowered MAP was increased to 85.6% of the baseline by the whole blood injection. In the rHSA-FecycP and rHSA-FepivP groups, the decreased MAP was elevated to 70.1 and 71.4% of the basal values (80.7 and 87.1% of the values before the bleedings).

The HR and respiration rate had decreased to 88.6–97.4 and 76.5–82.5% of the baselines by the 30% bleeding [Fig. 2(b,c)]. Both parameters returned to the initial levels by the injection of rHSA-FecycP, rHSA-FepivP, and whole blood within 30 min.

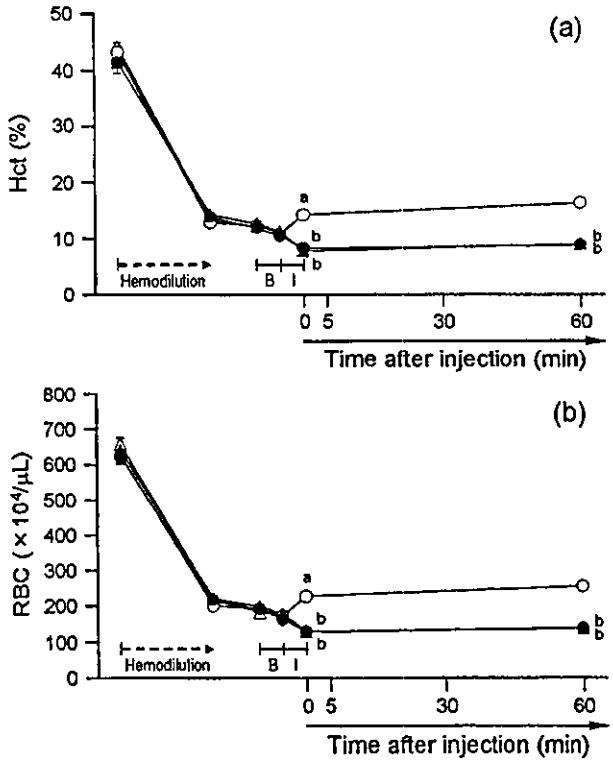

Figure 1. Effect of rHSA-heme solutions on Hct (a), and RBC numbers (b) in anesthetized rats subjected to hemodilution and hemorrhage. Each value represents the mean ± SEM of six rats (●, rHSA-FecycP group; ▲, rHSA-FepivP group; ○, whole blood group; and △, rHSA group). B, bleeding; I, sample injection. $^{a}p < 0.05$ versus rHSA group. $^{b}p < 0.05$ versus whole blood group.

ptO_2(R) and ptO_2(M)

After the 30% bleeding, ptO_2(R) decreased to 59.9–77.3% of the baseline [Fig. 3(a)]. Whereas the iv administrations of rHSA solution did not show restoration, the injection of the rHSA-FecycP, rHSA-FepivP, or whole blood immediately increased the ptO_2(R) level to 84.1–94.8% of the baselines (102.1–112.3% of the values before the bleeding). They remained unaltered by the end of the measurements.

The ptO_2(M) had also decreased to 49.4–52.9% of the basal value after the isovolemic hemodilution, and further decreased to 12.1–26.7% because of the 30% bleeding [Fig. 3(b)]. The iv administration of the whole blood increased the ptO_2(M) to 62.8% of the baseline after 60 min. In the rHSA-FecycP and rHSA-FepivP groups, the increasing ratios were relatively small: 34.2 and 36.9% of the baselines (76.2 and 66.8% of the values before the bleedings).

Blood gas parameters

The paO_2 increased to 111.3–123.2% of the baseline after the isovolemic hemodilution, and reached 148.0–153.6% after the 30% bleeding [Fig. 4(a)]. The injection of the whole blood showed a significant effect for restoration. Nonetheless, the recoveries by the albu-

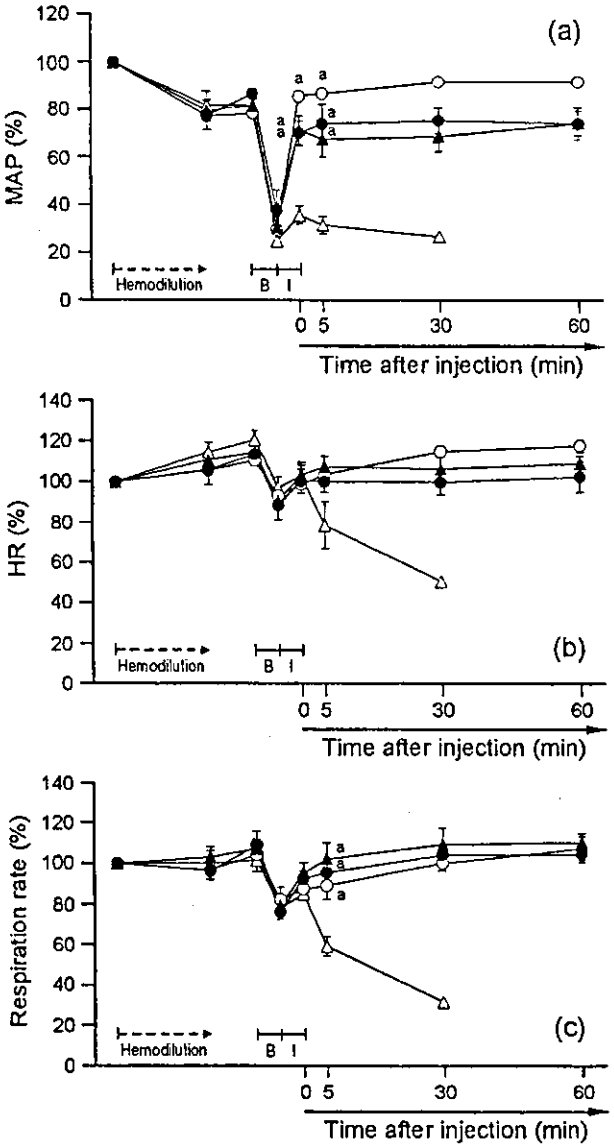

Figure 2. Effect of rHSA-heme solutions on MAP (a), HR (b), and respiration rate (c) in anesthetized rats subjected to hemodilution and hemorrhage. Each value represents the mean ± SEM of six rats (●, rHSA-FecycP group; ▲, rHSA-FepivP group; ○, whole blood group; and △, rHSA group). B, bleeding; I, sample injection. $^{a}p < 0.05$ versus rHSA group.

min-heme solutions were almost to the same extent as that seen in the rHSA group.

The pvO_2 decreased to 56.5–69.8% of the basal value after the 30% bleeding. The low value was not improved by the iv administration of 5 g/dL rHSA [Fig. 4(b)]. In contrast, the infusions of rHSA-FecycP, rHSA-FepivP, and whole blood immediately increased pvO_2 to 88.9–94.8%.

The changes in pH showed the same profile in all groups until 60 min after injection [Fig. 4(c)]. The pH of 7.39–7.42 was slightly increased to 7.47–7.49 after the bleeding and reduced to 7.34–7.37 by the administration of the samples, which slowly returned close to the initial level except for the rHSA-FecycP group.

The $paCO_2$ decreased to 66.3–73.9% of the basal value after the 30% bleeding. The iv administration of whole blood immediately increased it to 95.1% [Fig. 4(d)]. The recovery by the infusion of the rHSA-FecycP or rHSA-FepivP solution was relatively small (80.9–88.0%).

DISCUSSION

In this study, animals were anesthetized with sevoflurane, which is widely used in clinical situations. We had evaluated the oxygen-transporting ability of rHSA-FepivP using a similar acute anemia model with pentobarbital as an anesthesia.[21] Most of the parameter changes showed the same extent as those observed in the former experiment, except for the small degree of $ptO_2(R)$ reduction after the bleeding (32%) (50% decrease in the former study). It is probably attributable to the difference in the blood exchanging ratio.

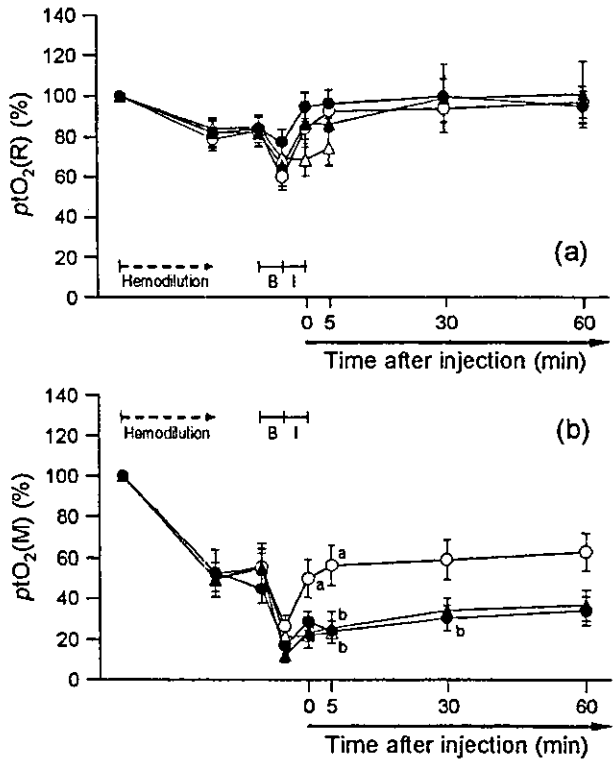

Figure 3. Effect of rHSA-heme solutions on the $ptO_2(R)$ (a) and $ptO_2(M)$ (b) in anesthetized rats subjected to hemodilution and hemorrhage. Each value represents the mean ± SEM of six rats (●, rHSA-FecycP group; ▲, rHSA-FepivP group; ○, whole blood group; and △, rHSA group). B, bleeding; I, sample injection. $^{a}p < 0.05$ versus rHSA group. $^{b}p < 0.05$ versus whole blood group.

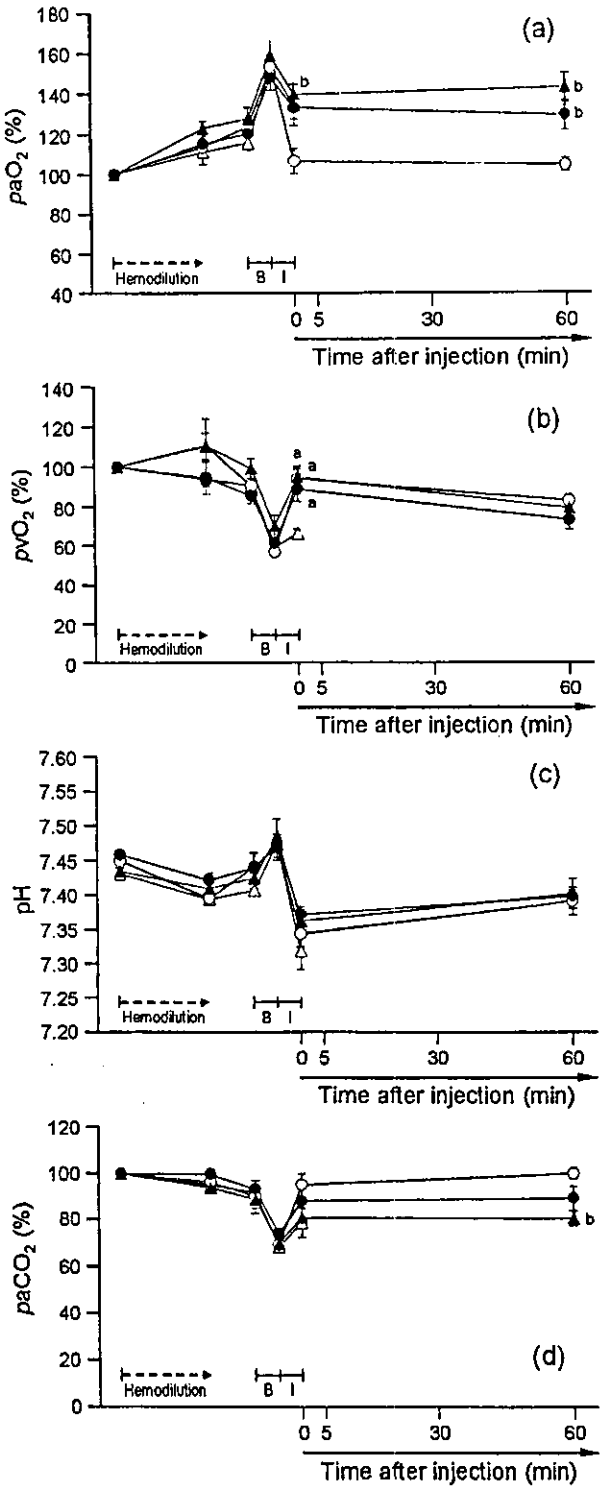

Figure 4. Effect of rHSA-heme solutions on paO_2 (a), pvO_2 (b), pH (c), and $paCO_2$ (d) in anesthetized rats subjected to hemodilution and hemorrhage. Each value represents the mean ± SEM of six rats (●, rHSA-FecycP group; ▲, rHSA-FepivP group; O, whole blood group; and △, rHSA group). B, bleeding; I, sample injection. $^b p < 0.05$ versus whole blood group. $^a p < 0.05$ versus rHSA group.

In the glass capillaries for the Hct determinations, the supernatant after centrifugation (12 kG, 5 min) was colored red by the homogeneously dispersed albumin-heme molecules without any aggregation. This indicates that the albumin-heme fluids have a good solubility with the blood components.

Acute anemia after 70% hemodilution

The quantitative changes in Hct and RBC numbers showed that the 70% hemodilution and 30% exchange transfusion were precisely controlled. In acute anemia, the oxygen supply centralizes in vital organs, and the muscle tissues become hypoxic by peripheral vasoconstriction. In fact, the ratio of ptO_2 reduction in the muscle tissues after hemodilution was significant compared with that observed in the renal cortex.

Hemorrhagic shock by 30% bleeding

Decreasing the circulation blood volume induced a significant reduction of MAP, ptO_2(R), ptO_2(M), pvO_2, and $paCO_2$. Among the vital organs, renal perfusion is first impaired because of redistribution of the systemic blood flow; therefore, ptO_2(R) is sensitive to a subtle change in the blood circulation and oxygen delivery. The decreased pvO_2 after the 30% bleeding implies a low oxygen saturation of Hb and increased oxygen extraction. The HR and respiration rate had also decreased from the initial values. However, paO_2 was increased to 153.6% (129.6 mmHg) of the baseline, which could be attributable to hyperventilation. The $paCO_2$ decreased to 70.3% of the baseline and the pH was increased to 7.48. A respiratory alkalosis by hyperventilation might overcome the metabolic acidosis effect.

Responses to administration with albumin-heme

In all groups, the pH levels decreased to 7.35 just after sample injections. The rapid increase in blood volume could improve the circulatory flows and wash out the lactate in the tissues.

By administration of the 5 g/dL rHSA solution, the MAP, HR, respiration rate, ptO_2(R), ptO_2(M), paO_2, pvO_2, and $paCO_2$ did not recover, leading to death within 32 min. In contrast, the infusion of whole blood improved these values to their initial levels except for ptO_2(M). In the rHSA-FecycP and rHSA-FepivP groups, the animals survived >60 min after the infusion, and the HR, respiration rate, ptO_2(R), and pvO_2 showed similar recoveries as observed in the whole

blood group. MAP, $ptO_2(M)$, paO_2, pH, and $paCO_2$ also returned, but not adequate relative to the whole blood group. We are certain that the albumin-heme solutions have the potential to (i) resuscitate the hemorrhagic shock, (ii) stabilize the blood circulation, and (iii) transport oxygen throughout the body. Nevertheless, the oxygen delivery to the peripheral tissues is still insufficient. The possible reasons were considered from the viewpoints of the physicochemical properties of albumin-heme.

Oxygen-binding affinity (p_{50}) (oxygen partial pressure in which 50% of Hb or albumin-heme is oxygenated)

It is known that an allosteric effect observed in the oxygen binding to Hb [the Hill coefficient (n) = 3.0] has implications for physiological use; the oxygen-transporting efficacy of RBCs between lungs [oxygen pressure (pO_2): 110 mmHg] and muscle tissues (pO_2: 40 mmHg) is estimated to be 22% at 37°C. The oxygen-equilibrium curve of albumin-heme does not show cooperativity; n is 1.0. However, the oxygen-binding affinity of albumin-hemes are adjusted somewhat low (rHSA-FecycP: p_{50} = 37 mmHg; rHSA-FepivP: p_{50} = 32 mmHg, respectively), so that they are able to show a similar oxygen-transporting efficacy of 22–23%.

Some investigators reported that a low p_{50} value is important to avoid the hypertensive effect; that is, the constrictive response is caused by excessive oxygen delivery to the arterioles.[10–13] McCarthy et al.[22] suggested that the increased oxygen delivery can be limited by increasing the molecular size, oxygen-binding affinity, and viscosity. Indeed, the PEG-conjugated Hb with a molecular weight of 90 kDa had no effect on the MAP.[23] However, Doherty et al.[24] denied this hypothesis based on their systematic experiments using recombinant Hbs (rHbs) with various p_{50} values; the small differences in the oxygen-equilibrium curves of the rHbs did not affect the magnitude of the pressor response. Our previous top-loading experiments using the albumin-heme solution (p_{50}: 32 mmHg) on the MAP changes and microcirculatory observations of the capillaries also showed that neither vasoconstriction nor hypertension occurred, because of its low permeability through the vascular endothelium.[18] Thus, the differences in p_{50} may not be essential.

Heme concentration

The heme concentration of the shed blood to use the exchange transfusion in the whole blood group was 5.3 m*M*. In contrast, the concentrations of the FecycP or FepivP in the rHSA-FecycP or rHSA-FepivP solutions were 2.7–2.8 m*M*. The low heme concentration of albumin-heme is probably related to insufficient oxygen delivery, which may result in the low recovery of $ptO_2(M)$.

Viscosity

It has been reported that an endothelial-derived relaxing factor (nitric oxide) is generated in response to the shear stress on the capillary wall.[25] Recently, maintenance of the plasma viscosity has been proposed as a crucial mechanism to preserve the shear force during microcirculation.[26] The prompt flow by the injection of the albumin-heme solution with low viscosity (1.1 cP) compared with blood (4.4 cP) may reduce the peripheral resistance and induce partial vasoconstriction, which would reduce the blood flow. The correct measurement of the cardiac output is necessary to interpret the pO_2 data and to assay the oxygen delivery.

In conclusion, all physiological responses to the exchange transfusion with albumin-heme in acute anemia reveal that this synthetic RBC substitute has the capability to resuscitate the hemorrhagic shock. A significant difference could not be found between the two types of albumin-hemes, rHSA-FecycP and rHSA-FepivP. This rHSA-based oxygen-carrying plasma expander will become a promising material for a new class of RBC substitutes. The safety and oxygen delivery of albumin-heme will be reported in a forthcoming article.

The authors are grateful to NIPRO Corp., for their supporting the oxygen-infusion project.

References

1. Chang TMS. Recent and future developments in modified hemoglobin and microencapsulated hemoglobin as red blood cell substitutes. Artif Cells Blood Substit Immobil Biotechnol 1997;25:1–24.
2. Tsuchida E. Perspectives of blood substitutes. In: Tsuchida E, editor. Blood substitutes: present and future perspectives. Lausanne, Switzerland: Elsevier Science; 1998. p 1–14.
3. Winslow RM. New transfusion strategies: red cell substitutes. Annu Rev Med 1999;50:337–353.
4. Squires JE. Artificial blood. Science 2002;295:1002–1005.
5. Keipert P, Chang T. Pyridoxylated-polyhemoglobin solution: a low viscosity oxygen-delivery blood replacement fluid with normal oncotic pressure and long term storage feasibility. Biomater Artif Cells Artif Organs 1988;16:185–196.
6. Schultz SC, Grady B, Cole F, Hamilton I, Burhop K, Malcolm DS. A role for endothelin and nitric oxide in the pressor response to diaspirin cross-linked hemoglobin. J Lab Clin Med 1993;122:301–308.
7. Moisan S, Drapeau G, Burhop KE, Rioux F. Mechanism of the acute pressor effect and bradycardia elicited by diaspirin crosslinked hemoglobin in anesthetized rats. Can J Physiol Pharmacol 1998;76:434–442.

Scheme 1. Synthetic Scheme of FeP-GluSu

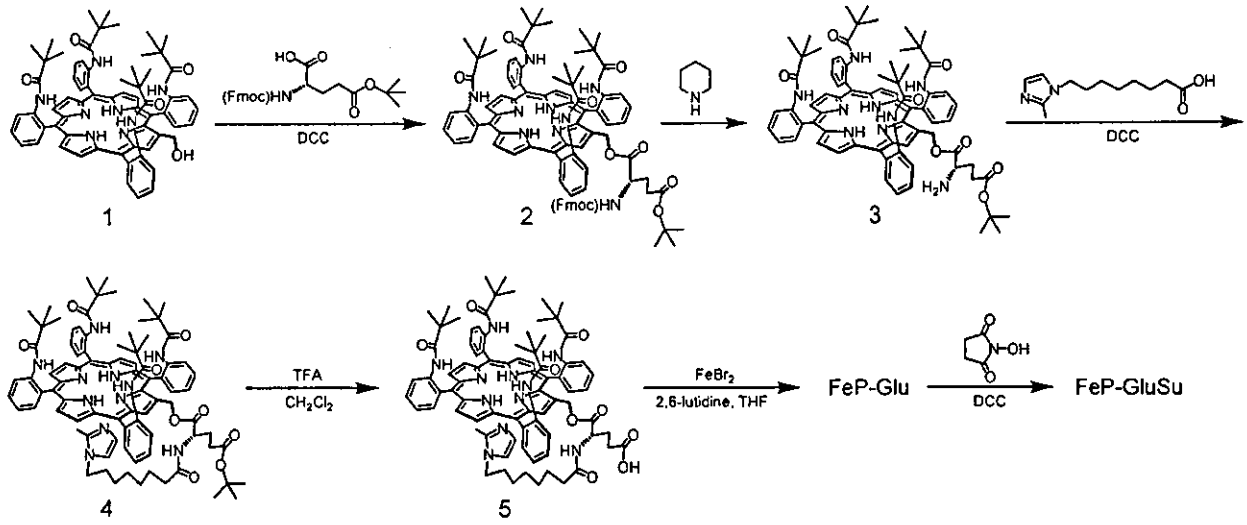

Table 1. CO-and O_2-Binding Parameters of rHSA(FeP-Glu) Conjugate in Phosphate-Buffered Solution (pH 7.3) at 25 °C

	$10^{-6}\,k_{on}^{CO}(M^{-1}s^{-1})$		$10^{-7}\,k_{on}^{O_2}(M^{-1}s^{-1})$		$10^{-2}\,k_{off}^{O_2}(s^{-1})$		$P_{1/2}^{O_2}$(Torr)[a]
system	fast	slow	fast	slow	fast	slow	
rHSA(FeP-Glu) conjugate	6.2	1.1	2.8	–	3.3	–	9 (27)
rHSA-FeP hybrid[b]	4.7	0.66	3.2	1.0	7.2	2.2	13 (35)
Hb(T-state)α[c]	0.22	–	0.29	–	1.8	–	40

[a] At 37 °C in parenthesis. [b] From ref 4c. [c] From refs 13–15.

First, Fmoc-L-Glu(g-*tert*-butyl ester) was bound to the OH group at the β-pyrrolic position of the porphyrin **1** by DCC. After removal of the Fmoc protecting group with piperidine, 8-*N*-(2-methylimidazolyl)octanoic acid was reacted with the obtained compound **3** in CH_2Cl_2, giving the imidazolyl-tailed porphyrin (**4**). The *tert*-butyl group was then removed by TFA, and the central iron insertion was carried out by the general $FeBr_2$ method to afford the iron-porphryin FeP-Glu. Finally, the reaction of *N*-hydroxysuccinimide with DCC gave the FeP-GluSu. All reactions can be performed at room temperature with high yields. The analytical data of all compounds described above were satisfactory obtained (*7*).

The FeP-Glu was converted to the ferrous complex by reduction in a heterogeneous two-phase system (toluene/aqueous $Na_2S_2O_4$) under an N_2 atmosphere (*6, 8*). The UV–vis absorption spectrum of the orange solution showed five-*N*-coordinated Fe(II) species (λ_{max}: 440, 531, 563 nm) via intramolecular imidazole binding (*6, 8, 9*). Upon exposure to CO, its UV–vis absorption immediately moved to that of the CO adduct complex. On the other hand, the dioxygenation was unstable at 25 °C, which is likely due to the presence of the neighboring glutamic acid proton.

The EtOH solution of the carbonyl FeP-GluSu (2 mL) was then injected into the phosphate-buffered solution of rHSA (8 mL, pH 7.3) (molar ratio 4/1), and the mixture was gently stirred for 1 h at room temperature. The solution was dialyzed against phosphate buffer (pH 7.3) to remove EtOH. The MALDI-TOFMS demonstrated a single molecular ion peak at *m/z* 70 643 (Figure 1). Attempts to measure the molecular weight of the rHSA-FeP hybrid, in which the FePs are noncovalently accommodated, failed using MALDI- and ESI-TOFMS; the molecular ion peak of rHSA (65 500) was only observable because the FePs are dissociated from the albumin during the ionization process (*10*). Therefore, we can conclude that the FeP-Glu is conjugated with rHSA

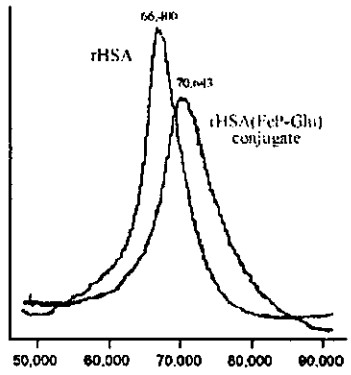

Figure 1. MALDI-TOFMS of the rHSA(FeP-Glu) conjugate. Matrix: 2,5-dihydroxybenzoic acid.

through amide bond formation. The average number of FeP-Glu in an rHSA was estimated to be 2.9–3.5, and this number is not dependent on the mixing molar ratio of FeP-GluSu/rHSA that ranged from 4 to 10. There are a total of 59 NH_2 groups in the rHSA structure, but only three of them are presumably active for the FeP-GluSu binding.

The conjugation of FeP-GluSu did not induce any change in the circular dichroism spectrum of rHSA in the 200–250 nm region. The Native PAGE of rHSA(FeP-Glu) also showed a single band with same migration distance of rHSA. Both results suggested that the secondary structure, molecular shape, and surface charge of albumin remained unaltered after the covalent binding of the hemes.

The UV–vis absorption spectrum of the rHSA(FeP-Glu) conjugate under an N_2 atmosphere showed a typical five-*N*-coordinated complex as seen in the toluene solution of FeP-Glu (Figure 2) (*4a,b, 6, 8, 9*). Upon exposure

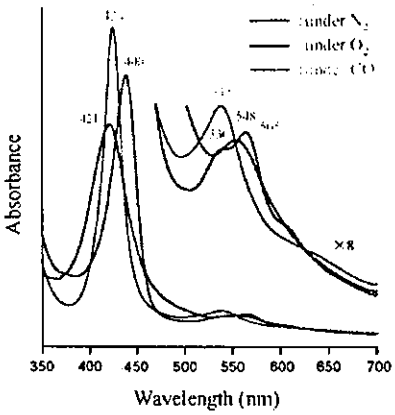

Figure 2. UV–vis absorption spectral changes of the rHSA-(FeP-Glu) conjugate in phosphate-buffered solution (pH 7.3) at 25 °C.

of this solution to O_2, the spectrum changed to that of the O_2-adduct complex under physiological conditions (pH 7.3, 37 °C) (*4a–c*). This dioxygenation was reversibly observed to be dependent on the O_2 partial pressure in the same manner as hemoglobin (Hb) and myoglobin. The half-lifetime of the O_2 adduct (ca. 5 h at 37 °C) was significantly longer than that of the noncovalent rHSA-FeP hybrid ($\tau_{1/2}$: 2 h) (*4d*). The covalent linkages of FeP-Glu to the protein scaffold obviously retarded the oxidation process of the central ferrous ion. Molecular simulation of the structure of FeP-GluSu revealed that the geometry of the imidazole ring against the porphyrin platform was perpendicular, which suggests that the spacer moiety between the imidazole and the porphyrin periphery does not produce an unfavorable distortion of the axial coordination and will not influence the O_2-binding behavior (see Chart 1b) (*11*).

The O_2-binding affinity [$P_{1/2}{}^{O_2}$] of the rHSA(FeP-Glu) conjugate was determined to be 27 Torr at 37 °C (*3b,c, 6, 7, 9, 10*), which is almost the same as that of the rHSA-FeP hybrid [$P_{1/2}{}^{O_2}$: 33 Torr] (*3b–d*) and identical to that of human red cells (*12*). The laser flash photolysis experiments provided the association rate constants of the O_2- and CO-bindings ($k_{on}{}^{O_2}$, $k_{on}{}^{CO}$) (*6, 8, 9a*). The absorption decays accompanying the O_2- and CO-recombination to the noncovalent rHSA-FeP hybrid were composed of two phases of the first-order kinetics, and the curves were fit by a double-exponential equation to determine k_{on} (fast) and k_{on} (slow) (Table 1) (*4c*). We supposed that the O_2- and CO-association to the FeP in the hydrophobic domains of the albumin was influenced by the molecular microenvironments around each O_2-coordination site, e.g., steric hindrance of the amino acid residue and difference in polarity (*4b–d*). The time dependence of the absorption change in the CO recombination to the rHSA(FeP-Glu) conjugate also showed double-exponential profile, but the rebinding process of O_2 obeyed monophasic decay. On the basis of studies on synthetic model hemes, it has been known that the proximal-side effect is the only primary factor which influences the association rate for CO but not for O_2 (*8, 9a*). We assume that there are two different geometries of the imidazole coordination and that each one shows the individual kinetics of the CO association. The covalent linkages between the axially coordinated imidazolyl side-chain and the albumin structure may provide an additional strain of the Fe–N(imidazole) bond and gives two conformations of the proximal-base binding. Since the $k_{on}{}^{O_2}$ value of rHSA(FeP-Glu) was nearly the same as the $k_{on}{}^{O_2}$ (fast) of the rHSA-FeP hybrid (Table 1), the FeP-Glu molecules are likely to locate on the surface of rHSA.

In conclusion, reaction of the newly synthesized tetrakis{(α,α,α,α-*o*-pivalamido)phenyl}porphinatoiron(II) with a proximal base and succinimidyl(glutamyl) group to rHSA produced a novel albumin conjugate bearing covalently attached heme groups as O_2-coordination sites. The molecular weight of rHSA(FeP-Glu) was directly measured by MALDI-TOF MS. In nature, one can find unique heme-linked proteins, e.g., cyctochrome *c*. The rHSA(FeP-Glu) conjugate presumably becomes a valuable model of these hemoproteins. The obtained rHSA-(FeP-Glu) can reversibly absorb O_2 under physiological conditions, and its O_2-binding affinity showed an identical value to that for human erythrocytes. These results suggest that this novel plasma protein may efficiently transport O_2 in the bloodstream as an O_2-carrier with a long circulation time.

ACKNOWLEDGMENT

This work was partially supported by Grant-in-Aid for Scientific Research (No. 16350093) from JSPS, Grant-in-Aid for Exploratory Research (No. 16655049) from MEXT Japan, and Health Science Research Grants (Regulatory Science) from MHLW Japan. R.M.W. acknowledges NNSFC (No. 20274034). The authors are grateful to NIPRO Corp. for their supporting the oxygen-infusion project.

Supporting Information Available: Experimental details of the compounds **2**, **3**, **4**, **5**, FeP-Glu, and FeP-GluSu and their spectroscopic data. This material is available free of charge via the Internet at http://pubs.acs.org.

LITERATURE CITED

(1) Peters, T., Jr. (1996) All about albumin. *Biochemistry, Genetics, and Medical Applications*, Academic Press, San Diego; and reference therein.

(2) Kragh-Hansen, U. (1981) Molecular aspects of ligand binding to serum albumin. *Pharmacol. Rev. 33*, 17–53.

(3) Curry, S., Brick, P., and Franks, N. P. (1999) Fatty acid binding to human serum albumin: new insights from crystallographic studies. *Biochim. Biphys. Acta 1441*, 131–140.

(4) (a) Komatsu, T., Hamamatsu, K., Wu, J., and Tsuchida, E. (1999) Physicochemical properties and O_2-coordination structure of human serum albumin incorporating tetrakis(*o*-pivamido)phenylporphyrinatoiron(II) Derivatives. *Bioconjugate Chem. 10*, 82–86. (b) Tsuchida, E., Komatsu, T., Matsukawa, Y., Hamamatsu, K., and Wu, J. (1999) Human serum albumin incorporating tetrakis(*o*-pivalamido)phenylporphinatoiron(II) derivative as a totally synthetic O_2-carrying hemoprotein. *Bioconjugate Chem. 10*, 797–802. (c) Komatsu, T., Matsukawa, Y., and Tsuchida, E. (2000) Kinetics of CO- and O_2-binding to human serum albumin-heme hybrid. *Bioconjugate Chem. 11*, 772–776. (d) Komatsu, T., Matsukawa, Y., and Tsuchida, E. (2002) Effect of heme structure on O_2-binding properties of human serum albumin-heme hybrids: intramolecular histidine coordination provides a stable O_2-adduct complex. *Bioconjugate Chem. 13*, 397–402. (e) Tsuchida, E., Komatsu, T., Hamamatsu, K., Matsukawa, Y., Tajima, A., Yoshizu, A., Izumi, Y., and Kobayashi, K. (2000) Exchange transfusion of albumin-heme as an artificial O_2-infusion into anesthetized rats: physiological responses, O_2-delivery and reduction of the oxidized hemin sites by red blood cells. *Bioconjugate Chem. 11*, 46–50. (f) Kobayashi, K., Komatsu, T., Iwamaru, A., Matsukawa, Y., Watanabe, M., Horinouchi, H., and Tsuchida, E. (2003) Oxygenation of hypoxia region in solid tumor by administration of human serum albumin incorporating synthetic hemes. *J. Biomed. Mater. Res. 64A*, 48–51. (g) Tsuchida, E., Komatsu, T., Matsukawa, Y., Nakagawa, A., Sakai, H., Kobayashi, K., and Suematsu, M. (2003) Human serum albumin incorporating synthetic heme: red blood cell substitute

without hypertension by nitric oxide scavenging. *J. Biomed. Mater. Res. 64A*, 257–261.

(5) Russo, S. M., Pepe, J. Y., Donohue, S., Cable E. E., Lambrecht, R. W., and Bonkovsky, H. L. (1995) Tissue distribution of zinc-mesoporphyrin in rats: relationship to inhibition of heme oxygenase. *J. Pharmacol. Exp. Ther. 272*, 766–774.

(6) Tsuchida, E., Komatsu, T., Ando, K., Kumamoto, S., and Nishide, H (1995) Synthesis and O_2-binding properties of tetraphenylporphyrinatoiron(II) derivatives bearing a proximal imidazole covalently bound at the β-pyrrolic position. *J. Chem. Soc., Perkin Trans. 2* 1995, 747–753.

(7) The synthetic details and spectroscopic data of the porphyrins can be obtained from the Supporting Information.

(8) Tsuchida, E., Komatsu, T., Arai, K., and Nishide, H. (1993) Synthesis and dioxygen-binding properties of double-sided porphyrinatoiron(II) complexes bearing covalently bound axial imidazole. *J. Chem. Soc., Dalton Trans.* 2465–2469.

(9) (a) Collman, J. P., Brauman, J. I., Collins, T. J., Iverson, B. L., Lang, G., Pettman, R. B., Sessler, J. L., and Walters, M. A. (1983) Synthesis and characterization of the "Pocket" porphyrins. *J. Am. Chem. Soc. 105*, 3038–3052. (b) Collman, J. P., Brauman, J. I., Iverson, B. L., Sessler, J. L., Morris, R. M., and Gibson, Q. H. (1983) O_2 and CO binding to iron(II) porphyrins: a comparison of the "Picket Fence" and "Pocket" porphyrins. *J. Am. Chem. Soc. 105*, 3052–3064.

(10) Tsuchida, E., Komatsu, T., and Yanagimoto, T. (2000) Molecular environment effect on O_2-binding to lipidporphyrinatoiron(II) complexes in aqueous media, *J. Porphyr. 4*, 81–87.

(11) The esff force field simulation was performed using an Insight II system (Molecular Simulations Inc.). The structure was generated by alternative minimizations and annealing dynamic calculations from 1,000 K to 100 K.

(12) Severinghaus, J. W. (1966) Blood gas calculator. *J. Appl. Physiol. 21*, 1108–1116.

(13) Sawicki, C. A., and Gibson G. H. (1977) Properties of the T State of Human Oxyhemoglobin Studied by Laser Photolysis. *J. Biol. Chem. 252*, 7538–7547.

(14) Sharma, V. S., Schmidt, M. R., and Ranney, H. M. (1976) Dissociation of CO from Carboxyhemoglobin. *J. Biol. Chem. 251*, 4267–4272.

(15) Steinmeier, R. C., and Parkhurst, L. J. (1975) Kinetic Studies on the Five Principle Components of Normal Adult Human Hemoglobin. *Biochemistry 14*, 1564–1573.

BC049859M

第12節　人工赤血球

1. 酸素輸液の必要性

輸血システムの確立により，輸血用血液が普遍的に常備されるようになり，医療の進展に大きな貢献をしてきた。輸血にともなう感染の確率は，核酸増幅法など献血液の厳重な検査と管理によって著しく低下してはいる。だが，未知の感染源の可能性も考えると，完全に零とはいえない。加えて赤血球の保存期限はわずか3週間である。献血1回当たりの採血量は400 mlになったが，人口の高齢化にともない健康な献血者総数は低下しつづけている。わが国のように自然災害が危惧される場合，緊急需要に対応した大量保存は重要な国家的施策でもある。血液型に関係なく要請に即応して，いつでもどこでもただちに供与できる，酸素輸液(人工赤血球)の出現が強く期待されている(図1)。

2. ヒトヘモグロビン小胞体の構成

酸素輸液の開発は歴史的には粗製ヘモグロビン(Hb)の投与(1916年)に始まる。現在は修飾Hb(分子内架橋型，重合型，高分子結合型など直接Hbを加工)の臨床試験が進行中である。しかし，修飾Hb溶液系では血管収縮による血圧亢進，代謝異常，軽度の神経毒性など，赤血球とかけ離れた構造に起因する副作用が指摘されている。Hb

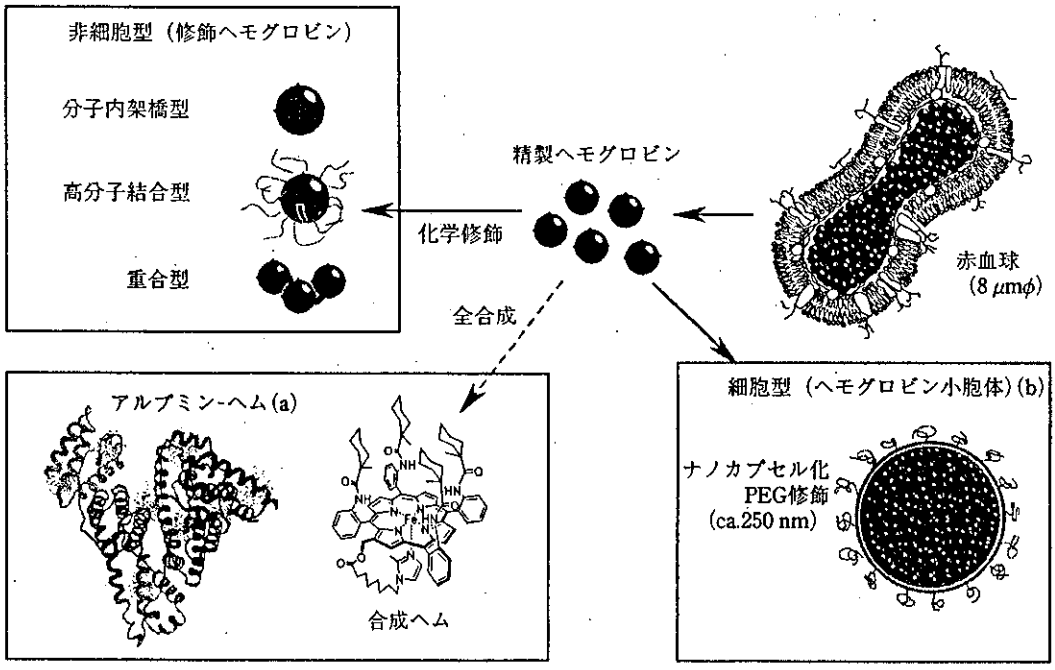

精製ヘモグロビン利用の非細胞型(a)と細胞型(b)のヘモグロビン小胞体，また合成ヘム誘導体を利用するアルブミン-ヘムが開発されている。

図1　酸素輸液の開発動向

が赤血球内にある理由は，①35％濃厚Hb溶液の高い粘度と膠質浸透圧の抑制，②本来毒性を有するHbの逸脱の抑制，③Hb機能維持のための各種リン酸などエネルギー分子，解糖ならびに還元－酵素系の保持である。また，④血液(血球分散系)は非ニュートン流体で，体内循環とくに末梢血管内における，特色ある流動形式と生理作用の特性を示す。赤血球構造を考えると，Hbを無害なカプセルに入れた細胞型のHb小胞体が有効である[1]。粒径制御とリン脂質が構成する2分子膜で高濃度Hb溶液を被覆する課題は，筆者らによって達成された。高純度高濃度の精製Hb溶液を用い，またextrusion法の採用により，Hb溶液(濃度35％以上)がほぼ1枚膜に包まれた，Hb小胞体の製造に成功した。ウィルス不活化と滅菌の困難も，Hbに一酸化炭素(CO)を結合して安定化させ60～70℃の加熱で完了した。最終段階で光照射励起により，酸素を結合したHbO_2に変換する。またアロステリック因子を共存させて，酸素親和度の制御(9～60 Torr)ができる。Poly(ethyleneglycol)(PEG)結合脂質を粒子表面に配置して，小胞体粒子間の凝集抑制と分散安定度向上の効果を観測し，この表面修飾過程を動力学的に明らかにし，溶液のまま室温にて2年以上保存できる系が構築されている。

3. ヘモグロビン小胞体の投与試験

Hb小胞体の動物投与試験では，90％超の高度交換輸血の場合でも，循環動態保持が確認されている[2),3)]。小胞体表面をPEG修飾すると，小胞体凝集を抑制でき，粘度と膠質浸透圧はほぼ血液と同等の非ニュートン流体になる。80％交換輸血における皮下微小循環動態の検討では，血管内を流動するPEG修飾Hb小胞体に凝集は認められず，血漿相に均一分散している[4)]。他方，未修飾群は細静脈や毛細管内で凝集体が観測されている。血流速度，有効毛細管密度，組織酸素分圧ともにPEG修飾系が，未修飾の系に比較しきわめて高い値に推移し，PEG修飾が不可欠であることが確認できた。

Hb小胞体の安全性についても明らかになっている。Hb小胞体は最終的に脾，肝に移行するが，貪食細胞に捕捉されたHb小胞体は7日以内に分解消失することが，組織病理学的に確認されている[5)]（図2)。細網内皮系の貪食機能は変動するが，可逆的であり，一過性で血液生化学的検査の結果

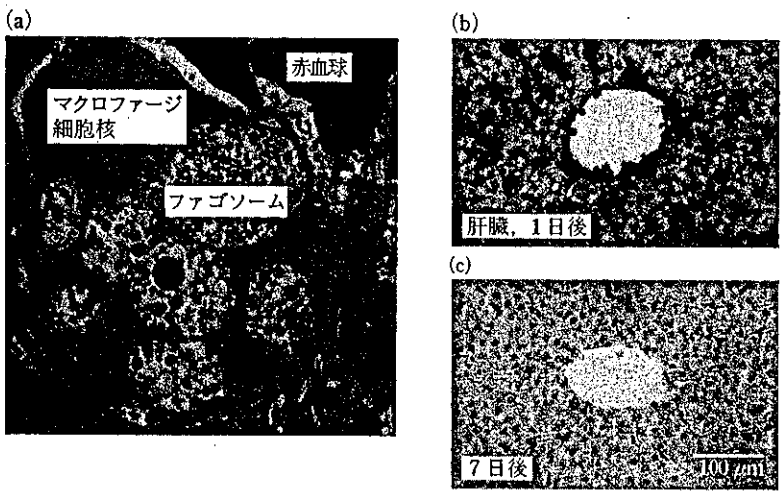

(a) Hb小胞体投与1日後のラット脾臓マクロファージの透過型電子顕微鏡写真。食胞（ファゴソーム）中にHb小胞体の粒子が多数認められる。この後3日目には消失する。(b)(c) Hb小胞体投与後のラット肝臓の抗ヒトHb抗体染色後の顕微鏡写真。色の濃い部分がヒトHbの存在部位。投与1日後では多量のHbの存在（Kuppfer細胞内）が認められるが，投与7日後にはほとんど消失，蓄積を認めない。

図2　ヘモグロビン小胞体の代謝過程

からも臓器の異常は認められていない。

修飾Hb投与に際し血圧の異常亢進や，血管床への血小板沈着などの副作用が認められている。これはNOとの高い親和性に起因する。とくに分子内架橋Hbはきわめて小さい(7 nm)ため，血管内平滑筋近傍に接近し，内皮細胞由来NOを捕捉し，血管弛緩機能を低下させる。血管収縮は末梢循環と組織酸素化を阻害する。他方，直径250 nmのHb小胞体では血管外漏出はなく，また血管平滑筋まで接近せず，NO結合反応は抑制され，血管収縮も血圧亢進も起こらない[6]。

肝臓中ではhemeoxygenaseが産生する一酸化炭素(CO)が，血管弛緩因子として作用する。摘出肝灌流実験では，Hb溶液はDisse腔に侵入し，Hbの代謝異常によるbilirubin排泄の亢進，またCOが血中Hbに捕捉され20％の血管抵抗増大を示し，同時に類洞の不連続的狭窄と流動停止領域の存在を確認している。他方，Hb小胞体はDisse腔に侵入できないため，この現象は生起しない[7,8]。

4. ヘムタンパク質系酸素輸液

他方，全合成型の酸素輸液の開発も進んでいる[9,10]。血清アルブミン(Mw. 66.5 kD)は血漿タンパク質の約70％を占める単純タンパク質であり，コロイド浸透圧の維持，各種内因性物質・薬物の運搬，血液pHの調整などの役割を果たしている。わが国では世界に先駆けて，遺伝子組み換えヒト血清アルブミン(rHSA)の，世界初の上市を間近に迎える状況にある。筆者らはこのアルブミンの非特異的多分子結合能を利用し，rHSAに酸素配位能を有するヘム誘導体を包接させる方法により，新しいアルブミン－ヘム(合成ヘムタンパク質)の創製に成功した。アルブミン－ヘムは，①完全合成系酸素輸液であり，感染の危険性がまったくない，②一切のヒト(および動物)由来の血液資源を必要としない，③酸素親和度(P_{50})はヘム構造の調整により調節可能，④アルブミンが血管内皮を透過しないため，NO捕捉にともなう血管収縮・血圧亢進は惹起されない，などの優れた特徴をもつ。すでに酸素輸液としての酸素結合能，溶液物性，血液適合性が実証されており，安全性と効果の解明を中心とした前臨床評価試験が進められている。

アルブミン1分子当たりに結合するヘムの数は最大8，これはHbの2倍に相当する。包接の駆動力は疎水性相互作用であるため，結合後もアルブミンの二次構造や表面電荷に変化はないと考えられてきた。だが，ごく最近S. Curry (Imperial College)らは，脂肪酸包接rHSAのX線結晶構造解析に初めて成功し，基質結合後のrHSAは幅8 nmから9 nmへ膨張することを明らかにした[11]。この発見はヘムがrHSA内部に包接されると，分子レベルで構造変化が誘起されることを示唆しており，酸素配位特性の変化とも関連して，アルブミン－ヘム結晶構造の解明が待たれている。

また酸素配位結合部位であるヘムの化学構造(酸素配位座近傍置換基，分子内軸塩基など)を変化させた一連の誘導体群が合成され，rHSA包接体とした系について，ヘム構造と酸素配位能の相関が定量的に明らかにされている[12,13]。

アルブミン－ヘムのNO親和度はO_2親和度の7.6×10^6倍と高いが[14]，体内へ投与しても，非細胞型Hbに見られる血管内皮からの漏出，NO捕捉にともなう血圧亢進は認められない(図3)。これはアルブミンの表面電荷が負に帯電していることに起因する。

さらにアルブミンのCys^{34}をビスマレイミド誘導体で架橋する方法により，アルブミン二量体が

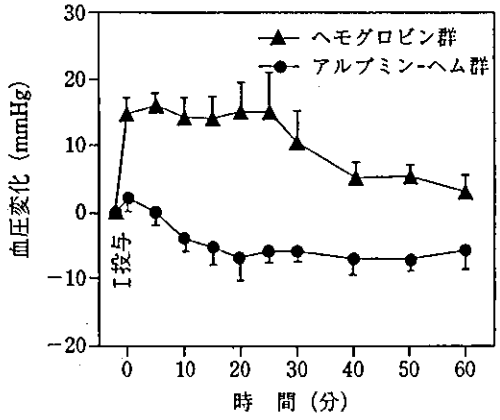

ヘモグロビン投与ではただちに血圧が上昇するが，アルブミン-ヘムではそのような現象は認められない。

図3　アルブミン-ヘム溶液をラットに投与した後の血圧変化

合成され，それにヘム16分子が結合されたアルブミンーヘム二量体[15]も完成している。この10 wt％水溶液はコロイド浸透圧を生理条件に保った条件で，血液の1.3倍量の酸素を溶解できる。

5. おわりに

酸素輸液の研究は，このようにこの20年間で具体的対象物についての物性と動的機能の相関が詳しく解明できるようになっている。①型物質や感染源をまったく含まない，②浸透圧や粘度などの溶液物性が血液と同等に調節可能，③毒性がきわめて低く，ヒト血液換算で2～3 lit. 投与の場合でも安全かつ代謝可能，④長期保存(室温，2年間）と安価供給が可能などの特性を有する，酸素輸液の実現が間近といってよい。

【参考・引用文献】

1）E. Tsuchida., ed.：Blood substitutes, present and future perspective. Elsevier, Amsterdam, (1998).
2）Y. Izumi, et al.：*Crit Care Med*, **24**, 1869-1873 (1996).
3）H. Sakai, et al.：*Bioconjugate Chem*, **8**, 23-30 (1997).
4）H. Sakai, et al.：*J. Biomed Mater Res*, **40**, 66-75 (1998).
5）H. Sakai, et al.：*Am. J. Phathol*, **159**, 1079-1086 (2001).
6）H. Sakai, et al.：*Am. J. Physiol Heart Circ Physiol*, **279**, 908-915 (2000).
7）N. Goda, et al.：*J. Clin. Invest*, **101**, 604-612 (1998).
8）T. Kyokane, et al.：*Gastroenterology*, **120**, 1227-1240 (2001).
9）E. Tsuchida, et al.：*Bioconjugate Chem*, **8**, 534-538 (1997).
10）T. Komatsu, et al.：*Bioconjugate Chem*, **10**, 82-86 (1999).
11）S. Curry, et al.：*Nature Struc. Biol*, **5**, 827-835 (1998).
12）T. Komatsu, et al.：*Bull. Chem. Soc. Jpn*, **74**, 1695-1702 (2001).
13）T. Komatsu, et al.：*Bioconjugate Chem*, **13**, 397-402 (2002).
14）T. Komatsu. et al.：*Bioconjugate Chem.*, **12**, 71-75 (2001).
15）T. Komatsu, et al.：*Macromolecules*, **32**, 8388-8391 (1999).

＜土田　英俊／武岡　真司／小松　晃之／酒井　宏水＞

日本表面科学会創立25周年記念
新訂版・表面科学の基礎と応用

発行日　2004年　6月　22日　初版第1刷発行

編者　日本表面科学会「新訂版・表面科学の基礎と応用」編集委員会

発行者　吉田　隆

発行所　株式会社 エヌ・ティー・エス
〒113-8755　東京都文京区湯島2-16-16
TEL:03(3814)3511(代表)　03(3814)9151(営業部)
http://www.nts-book.co.jp/

制作　編集室 アイ・ティ・オウ

印刷　ショウワドウ・イープレス株式会社

製本　牧製本印刷株式会社

ISBN4-86043-051-4　C3050

酸素輸送合成ヘム蛋白質“アルブミン-ヘム”の創製と酸素輸液の展開

小松 晃之・土田 英俊

早稲田大学 理工学総合研究センター

1. はじめに

ヒト血清アルブミン（HSA）は 血液のコロイド浸透圧調節に加え、種々の内因性・外因性物質を結合・輸送する役割を担う血漿蛋白質である。もし、この HSA にヘモグロビン(Hb)の酸素輸送能を付与することができれば、人工酸素運搬体（酸素輸液）としての利用価値はきわめて高く、例えば救急医療現場における救命措置への適用を考えただけでも、その絶大な有用性が容易に想像できる。

我々はHSA の非特異的多分子結合能に着目し、一連の近位塩基結合型ヘム（Figure 1）を遺伝子組換え HSA に包接させた人工のヘム蛋白質“アルブミン-ヘム(rHSA-heme)”を合成、それが生理条件下で Hb と同じように酸素を吸脱着できる酸素運搬体として機能する(酸素輸液となる)こと明らかにした[1-6]。ヘムはアルブミン 1 分子当たり最大 8 分子まで包接可能。得られた rHSA-heme 溶液の粘度、コロイド浸透圧、等電点はヘムの結合数によらず一定で、ヒト血液との適合性も高い[7]。また、酸素親和性はヘムの化学構造を変化させることにより調整できるなどの利点もある[5,6]。本報では、rHSA-heme の特徴と、それを利用した酸素輸液の展開について、最新の話題を紹介したい。

2. 酸素結合能

赤色の rHSA-heme 水溶液は室温で 2 年以上保存可能な安定度の高い製剤である。窒素雰囲気下における rHSA-heme 水溶液の可視吸収スペクトルパターンは、活性中心であるヘムが Fe(II) 5 配位高スピン錯体であることを示し、これは Hb の deoxy 体に相当する。そこへ酸素を通気すると速やかに酸素錯体(oxy 体)が形成され、その酸素結合解離は可逆的に観測できる。赤外吸収、共鳴ラマン、磁気円偏光二色性スペクトルから、酸素配位錯体の電子状態を詳細に解析した[2]。十数種類のヘム誘導体を対象に行った立体構造と酸素結合能の相関解明から、4 つのシクロヘキサノイル基を有するヘムを包接した rHSA 複合体が、最も安定な酸素錯体を形成できることを明らかにした[5]。酸素親和性(P_{50})は 30～36 Torr で赤血球(P_{50}: 27 Torr)に近く、酸素錯体半減期(τ_{50}: 9 hr)はミオグロビンの値に匹敵する。

3. 生体内投与後の血圧変化と微小循環動態

近年、修飾 Hb を利用した赤血球代替物が欧米を中心に具体化されてきているが、血管内皮弛緩因子である一酸化窒素の捕捉に伴う血圧亢進の回避が課題となっている[8-10]。rHSA-heme の一酸化窒素親和性を測定したところ、

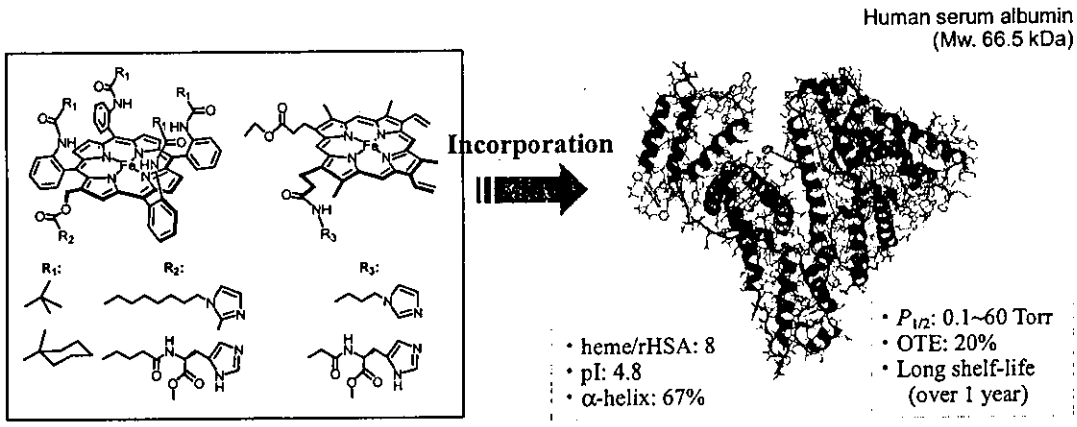

Figure 1 Synthetic hemes and simulated structure of rHSA-heme hybrid.

Hbより 9 倍高いことが明らかとなった[4]。つまり、rHSA-heme 分子が内皮細胞を透過して平滑筋近傍まで到達すると、瞬時に一酸化窒素を結合し、血管収縮を誘発する可能性がある。しかし予想に反し、rHSA-heme 溶液を静注したラットでは、血圧上昇は全く観測されなかった (Figure 2)[11]。rHSA-heme 溶液投与後の腸間膜細動脈径、細静脈径、血流速度にも変化は認められない。この理由はアルブミンの表面電荷にあると推察している。アルブミンは Hb に比べ等電点が低く(pI: 4.8)、内皮細胞を取り囲む基底膜との間に負電荷どうしの静電反発を生じるため、その血管内皮透過性は Hb の約 1/100 と低い。従って rHSA- heme の場合、投与後の急激な血圧上昇がないと考えられる。

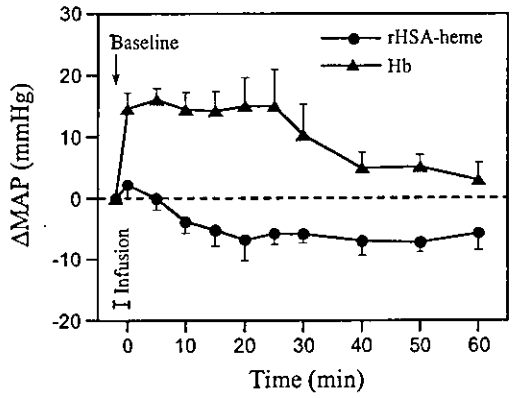

Figure 2 Changes of mean arterial pressure (MAP) after administration of rHSA-heme solution in anesthetized rats.

4. 脱血ショックモデルにおける生体内酸素輸送

麻酔下ラット脱血ショックモデルを作成し、rHSA-heme の *in vivo* 酸素運搬能を定量した[12]。まず全血液量の 70%を rHSA で希釈後、さらに全血液量の 30%を脱血、直ちに同量の rHSA-heme または rHSA を静注し、投与 2 時間後までの血液ガス、循環系パラメーター、腎皮質酸素分圧 (PtO_2(R)) を測定した。平均血圧 (MAP) は 30 %脱血後には 25-38 %まで減少、rHSA 群ではそのまま回復を認めることなく、投与 30 分以内に全例が死亡した (Figure 3)。一方、rHSA-heme 群では、投与直後に初期値の 70 % (脱血前値の 87%) まで上昇、本製剤が血圧回復に有効であることが明らかとなった。PtO_2(R) は 30%脱血直後に 60-77 %まで低下。rHSA のみの投与では回復は見られなかったが、rHSA-heme 群では、投与直後に 95 % (脱血前値の 115%) まで上昇し、2 hr 後でもその値は維持された。

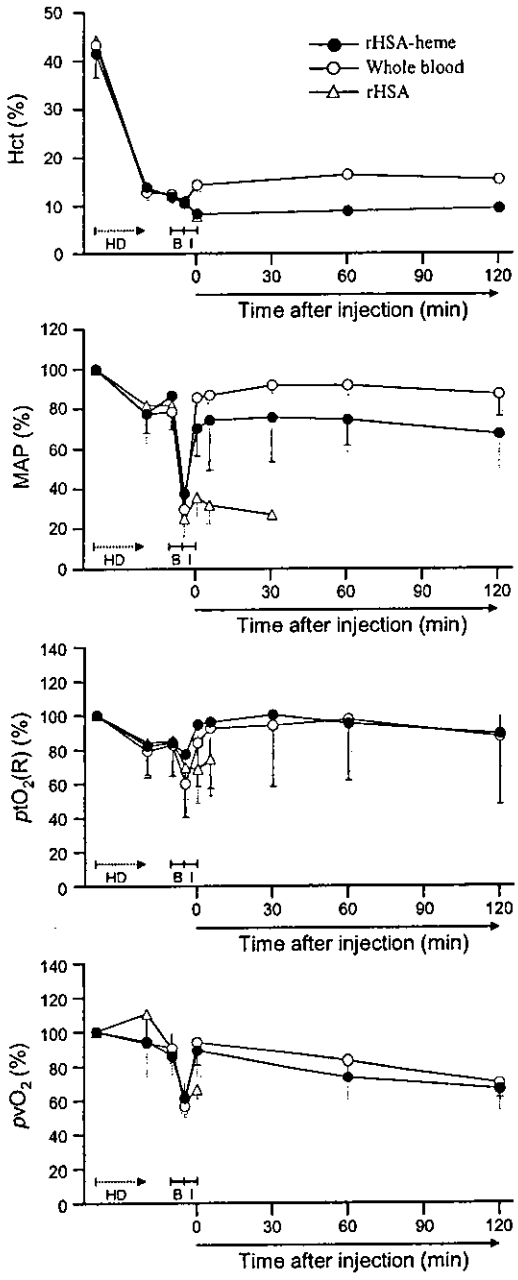

Figure 3 Changes of Hct, mean arterial pressure (MAP), renal cortical O_2-tension (ptO_2(R)), venous blood O_2-tension (pvO_2) after administration of rHSA-heme solution in anesthetized rats. HD: hemodilution with rHSA, B: 30% bleeding, I: sample infusion.